*ЖЭТФ, 1998, том 114, вып. 1(7), стр. 63–90* 

# HUND'S CASE (*a*)-CASE (*b*) TRANSITION IN THE SINGLET-TRIPLET ABSORPTION SPECTRUM OF PYRAZINE IN A SUPERSONIC JET

*E. S. Medvedev**

*Institute of Chemical Physics of Russian Academy of Sciences*
*142432, Chernogolovka, Moscow region, Russia*

*D. W. Pratt*

*Department of Chemistry, University of Pittsburgh, Pittsburgh*
*PA 15260, USA*

Submitted 6 January 1998

An analytical expression is derived for calculating the intensities of individual spin-rovibronic lines in the fully resolved gas phase electronic spectrum of a polyatomic molecule, in which one of the zero-order electronic states is a triplet state. The expression is employed to calculate the effect of fine structure splitting on the singlet-triplet absorption spectrum of pyrazine using the parameters available from experiment. A transition from Hund's coupling Case (*a*) to Case (*b*) on going from low $J$ to high $J$ rotational levels is predicted to occur at a moderate resolution of a few hundred MHz. The effect is more pronounced in pyrazine-$d_4$ and the pyrazine-argon van der Waals complex owing to their larger mass.

## 1. INTRODUCTION

The pyrazine molecule continues to attract much attention due to its unique photophysical properties. Owing to a moderate $S_1 - T_1$ energy gap (4056 $cm^{-1}$), the density of $T_1$ vibrational levels at the $S_1$ origin is relatively low, which places pyrazine into the class of so-called intermediate-case polyatomic molecule [1] with respect to $S_1 - T_1$ intersystem crossing (ISC). In intermediate-case molecules, the coupling between the $S_1$ and $T_1$ states results in a formation of mixed singlet-triplet levels. These mixed levels have been revealed in ultrahigh resolution spectra and are believed to be responsible for observed nonexponential fluorescence decay behavior [2–7]. While the singlet states that participate in this mixing are well characterized, little is known about the zero-order triplet states. The important point, in particular, is that the effect of the fine structure splitting on the triplet state energy level structure of the gas phase molecule is not well understood, even at the $T_1$ origin.

In solid matrices at liquid helium temperatures, the energy of the lowest triplet state is split into three spin sublevels $T_x$, $T_y$ and $T_z$, each having very different phosphorescence lifetimes $\tau_x$, $\tau_y$ and $\tau_z$. The separations and lifetimes of these sublevels in pyrazine have been measured by the microwave-induced delayed phosphorescence (MIDP) technique [8–12]. Figure 1 shows the sublevel ordering and microwave transitions observed [9] in a benzene crystal at 1.2 K together with the appropriate choice of molecular axes. The lifetimes measured in different media are listed in Table 1.

*E-mail: medvedev@landau.ac.ru

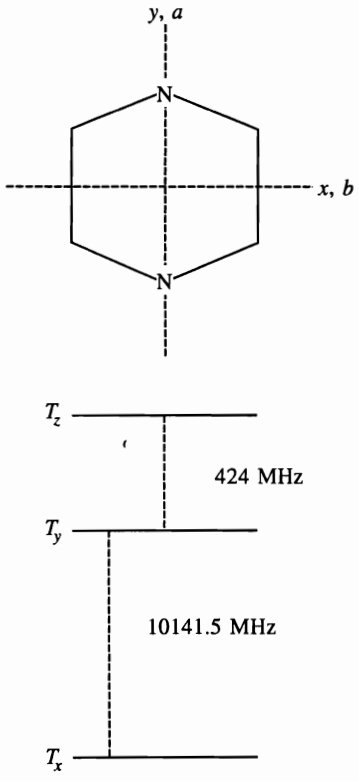


**Fig. 1.** Ordering and energy level separations of the lowest triplet state of pyrazine in the solid state, as obtained from MIDP experiments. The smallest moment of inertia in the gas phase is about the N-N line (the $a$ axis) in both the $S_0$ and $T_1$ states. The largest moment of inertia is about the axis perpendicular to the molecular plane, the $z$ ($c$) axis of the top

*Table 1*

**Triplet spin sublevel lifetimes of the lowest triplet state of pyrazine***

| | $\tau_x$ | $\tau_y$ | $\tau_z$ | Ref. |
|---|---|---|---|---|
| Benzene host crystal at 1.2 K | 6.3 | 284 | 163 | [9] |
| *Para*-dioxane host crystal at 1.6 K | 6.5 | 400 | 200 | [11] |
| Supersonic jet | $\tau_{ph}$ = 1.45 (upper limit 2.5) | | | [27] |

* All values in msec.

In the MIDP experiments, the $T_1$ state is prepared in an indirect way *via* $S_1 \leftarrow S_0$ excitation followed by $S_1 \rightarrow T_1$ ISC. The direct $T_1 \leftarrow S_0$ electronic transition in pyrazine also has been observed in the absorption spectra of solids [13–15] and vapors [16–18]. The measured oscillator strengths were determined to be $10^{-7}$ and $3 \cdot 10^{-8}$, respectively, [18], which is typical of a spin-forbidden transition. In supersonic jets, the $T_1 \leftarrow S_0$ transition was first detected using the multiphoton ionization (MPI) method [19] and then by phosphorescence excitation methods [20–27], in some cases using SEELEM (surface electron ejection by laser excited metastables) detection. Valuable information about the vibrationally excited $T_1$ state has also been obtained with the pulse-field-ionization technique [28].

As can be seen from Fig. 1 and Table 1, the $T_y$ and $T_z$ sublevels in the solid host are nearly degenerate and have similar lifetimes, whereas the $T_x$ sublevel is set apart by about 10 GHz and has a much shorter lifetime. While this phenomenon is well established in the condensed phase, no conclusive evidence for its manifestation in the gas phase molecule is available. Theoretically, it was explained in terms of the properties of spin-orbit coupling in aromatics and heteroaromatics with their characteristic $\pi$-electronic structure and planar geometry [29–34]. Since the planarity of the two participating states has been shown to survive in the gas phase [23], this phenomenon can be expected to occur in the gas phase, too, [25, 26]. However, the previous studies were performed at relatively low resolution ($\sim$ 2 GHz) [25, 26], not high enough to answer the question definitely.

Two additional factors complicate the interpretation of a gas phase experiment. The first is the lack of a condensed phase environment. If $\tau_x$, $\tau_y$ and $\tau_z$ are assumed to be the same in the solid and gas phases, then in jets a mean lifetime $\tau_{ph}$ arising from rotational mixing of the spin sublevels would be observed, which at least would not be shorter than the shortest lifetime in solids; i.e., 6.3 ms [9, 11]. The measured gas phase phosphorescence lifetime at the $T_1$ origin in a supersonic expansion is only 1.45 ms, with an upper limit of 2.5 ms [27] having been established in a separate experiment. Clearly, then, the environment plays a role. With the quantum yield of phosphorescence emission as large as 0.3 in a solid solution at 77 K [35], this implies that acceleration of radiative and nonradiative transitions to the ground state might both be responsible for the lifetime shortening in the jet. If, further, we accept the absolute values of the $T_1 \leftarrow S_0$ oscillator strengths cited above, which tell us that the oscillator strength is a factor of three lower in the gas phase than in a solid, then it is the nonradiative transition rate which is responsible for the lifetime shortening [27]. The reasons for this behavior are completely unknown.

The second factor complicating the interpretation of a gas phase spectrum are rotations which produce extensive mixing of the three spin sublevels of the triplet state. In the ground state, as well as in the lowest excited singlet and triplet states, the pyrazine molecule is a nearly symmetric top with rotational constants of about 3 and 6 GHz [26] (see Table 2). If in the gas phase the spin splittings are assumed to be on the same order of magnitude, 10 GHz, as in solids (which seems to be the case for glyoxal, where they change from 0.6 and 2.2 GHz to 1.1 and 2.4 GHz between the solid and gas phases, respectively [22]), then the nature of the spectrum will be quite different at low and high rotational quantum numbers.

*Table 2*

**Rotational and fine structure splitting constants of pyrazine in $cm^{-1}$ (values in parentheses are for pyrazine-$d_4$)**

| | $S_0$ | $T_1$ | Ref. |
|---|---|---|---|
| $A$ | 0.21285 | 0.212 | [26, 44] |
| | (0.18389) | | [44] |
| $B$ | 0.19767 | 0.196 | [26, 44] |
| | (0.17502) | | [44] |
| $C$ | 0.10249 | 0.101 | [26, 44] |
| | (0.08967) | | [44] |
| $D$ | | 0.3455 | [9, 44] |
| $E$ | | −0.00705 | [8, 43] |

For high values of the rotational angular momentum $N$, Hund's Case ($b$) should apply, in which case the spectrum should consist of rotational bands corresponding to transitions between states with definite values of the asymmetric rotor quantum numbers $N$, $K_{+1}$ and $K_{-1}$, each of which, exept for $N = 0$, is split into states with different values of $J = N$, $N \pm 1$, where $\mathbf{J} = \mathbf{N} + \mathbf{S}$ is the total angular momentum and $\mathbf{S}$ is the angular momentum of the spin. This is the analog of the rotational structure in the $\Sigma$ states of diatomic molecules which typically belong to Case ($b$) because of a weak spin-axis interaction [36, 37]. However, for low values of $N$, the observed bands will be shifted away from the purely rotational band positions since they are now spin-rotational bands. Again an analogy comes from diatomics whose $\Pi$, $\Delta$, etc. states usually belong to Case ($a$), apart from some light diatomics. The transition from Hund's Case ($a$) to Case ($b$) with increasing rotational quantum number is called spin uncoupling, of which several examples are given by Herzberg [36].

A general approach to calculating band intensities in the singlet-triplet spectra of polyatomic molecules was developed by Hougen [38], Creutzberg and Hougen [39], and di Lauro [40]. Energies and wavefunctions of spin-rotational levels of a triplet state were derived from an effective Hamiltonian given by Van Vleck [41] and Raynes [42]. The intensities of transitions in nearly symmetric tops were represented in the form of Hougen and di Lauro factors (rather than Hönl-London factors), tabulated for some limiting cases. The Hougen factors [38] are appropriate for a Hund's Case ($b$) molecule with no multiplet splitting in the triplet state. Creutzberg and Hougen further extended this approach to near-symmetric rotor molecules of symmetry $C_{2v}$, $D_2$, and $D_{2h}$, defining a new «limiting» Case ($ab$), which was further subdivided into types I, II, and III. Their Case ($ab$) corresponds to a situation, not unlike that of pyrazine in its lowest triplet state, in which two of the spin components of the nonrotating molecule are separated by a small energy, and the third is separated by a large energy, compared to the rotational interval. (In this respect, $T_1$ pyrazine is a Case ($ab$), type II molecule; thus we are actually dealing with a Case ($ab$) — Case ($b$) transition here.) The di Lauro factors are appropriate for all types of Hund's Case ($ab$) molecules; they account for the multiplet splittings by using Raynes' effective Hamiltonian [42] for asymmetric rotors which includes contributions from various magnetic interactions.

Here, we take a new approach to this problem, one that relies on the derivation of a closed-form analytical expression for the intensities, assuming arbitrary relations between rotational intervals, asymmetry and fine structure splittings. This approach is motivated by the likely success of future high resolution experiments on the singlet-triplet transitions of a wide variety of molecules, requiring a more general method for their interpretation. In the present instance, we make two simplifying assumptions, in order to make the problem tractable. Only the spin-spin interaction is taken into account [43, 44], and only one spin sublevel of the nonrotating molecule is assumed to be radiatively active [31]. A more general expression for the intensities is also obtained and compared with the Hougen factors [38]. We test our approach by computing the $T_1 \leftarrow S_0$ spectra of pyrazine, pyrazine-$d_4$, and the pyrazine-Ar van der Waals complex, for comparison with existing and future experimental spectra. The approach described here is extendable to other molecules, thereby anticipating new experiments in high resolution spectroscopy.

## 2. THEORY

### 2.1. Rotational States in $S_0$

Pyrazine has $D_{2h}$ symmetry in its ground ($S_0, {}^1A_{1g}$) and first excited triplet ($T_1, {}^3B_{1u}$) states. The smallest moment of inertia is about the axis passing through the two nitrogen atoms [23, 44]. Therefore, the rotational Hamiltonian for both $S_0$ and $T_1$ is of the form

$$H_r = BN_x^2 + AN_y^2 + CN_z^2, \tag{1}$$

where $A > B > C$ are the rotational constants (nearly the same in both states, see Table 2) and $N_{x,y,z}$ are the projections of the rotational angular momentum vector on the axes of the molecular coordinate frame (MCF), the inertial axes. For a symmetric top ($A = B$) without spin, the operators $\mathbf{N}^2, N_z$, and $N_{\tilde{z}}$, i.e., the rotational angular momentum squared and its projections on the $z$ axis of the MCF and on the $\tilde{z}$ axis of the laboratory coordinate frame (LCF), respectively, constitute a full set of commuting operators.

The electronic-vibrational-rotational (EVR) wavefunctions are written as

$$|\Gamma_S; NK\tilde{K}\rangle \equiv |\Gamma_S\rangle|NK\tilde{K}\rangle, \tag{2}$$

where $\Gamma_S$ (= $A_{1g}$ for the vibrationless $S_0$ state) is the symmetry species (IR, irreducible representation) of the electronic-vibrational wavefunction $|\Gamma_S\rangle$, $N$ is the rotational angular momentum quantum number, and $K$ and $\tilde{K}$ are the eigenvalues of $N_z$ and $N_{\tilde{z}}$, respectively. As a basis set for an asymmetric rotor without spin, we will use the symmetrized rotational wavefunctions that transform (under rotations by an angle $\pi$ with respect to the MCF axes) according to the IR's $\Gamma_r = A, B_1, B_2, B_3$ of the $D_2$ group,

$$|\Gamma_r \lambda \tau NK\tilde{K}\rangle = f_K 2^{-1/2}\left[|NK\tilde{K}\rangle + \tau|N, -K, \tilde{K}\rangle\right] \quad \text{for} \quad K \geq 0 \quad \text{and} \quad \tau = \pm 1, \tag{3}$$

where

$$f_K = 1 \quad \text{for} \quad K > 0 \quad \text{and} \quad f_K = 2^{-1/2} \quad \text{for} \quad K = 0. \tag{4}$$

In Eq. (3), two additional «quantum numbers», $\tau$ and

$$\lambda = \tau(-1)^N = \pm 1, \tag{5}$$

are defined for the characterization of the symmetrized basis functions. The reason for using $\lambda$ is that this is a «good quantum number» for the rotational, spin-spin, and spin-orbit Hamiltonians (see below). The relations between $\Gamma_r$ and $\lambda$ for different $K$ are shown in Table 3.

*Table 3*

**$K$ and $\lambda$ for irreducible representations of the $D_2$ group**

| $\Gamma_r$ | $\lambda$ | $K$ |
|---|---|---|
| $A$ | +1 | even |
| $B_1$ | −1 | even |
| $B_2$ | −1 | odd |
| $B_3$ | +1 | odd |

Since the asymmetric rotor Hamiltonian (1) has no matrix elements between the basis states (3) differing in either $\Gamma_r$, $\lambda$ or $\tau$, its eigenfunctions expanded in this basis can also be characterized by $\Gamma_r$, $\lambda$ and $\tau$ (in addition to $N$ and $\tilde{K}$),

$$|\Gamma_S\Gamma_r\lambda\tau Ni\tilde{K}\rangle = \sum_K C_K^{(\Gamma_S\Gamma_r\lambda\tau Ni)}|\Gamma_r\lambda\tau NK\tilde{K}\rangle, \tag{6}$$

where $i$ labels the eigenvalues of $H_r$ for a given $\Gamma_r$, $\lambda$, $\tau$ and $N$. Here $K$ runs from 0 to $N$ over all odd or even values depending on $\Gamma_r$ (see Table 3). The asymmetric top functions are labelled with $\Gamma_S$ because, unlike the case of the symmetric top, they are dependent on the rotational constants of the given electronic state. The eigenvalues and the coefficients $C_K^{(\Gamma_S\Gamma_r\lambda\tau Ni)}$ are found by diagonalizing $H_r$ in the basis (3). The Hamiltonian (1) conserves all quantum numbers except for $K$. Using the notation

$$\langle\Gamma_r\lambda\tau NK\tilde{K}|H_r|\Gamma_r\lambda\tau NK'\tilde{K}\rangle \equiv \langle K|H_r|K'\rangle,$$

we obtain the following nonvanishing matrix elements:

$$\langle K|H_r|K\rangle = \frac{1}{2}(A+B)\left[N(N+1) - K^2\right] + CK^2 \tag{7.1}$$

for $K \neq 1$,

$$\langle 1|H_r|1\rangle = \frac{1}{2}(A+B)\left[N(N+1) - 1\right] + C + \frac{1}{4}\tau(B-A)N(N+1) \tag{7.2}$$

for $K = 1$,

$$\langle K|H_r|K+2\rangle = \langle K+2|H_r|K\rangle = \\ = \frac{1}{4}(B-A)\left[(N-K)(N-K-1)(N+K+1)(N+K+2)\right]^{1/2} \tag{7.3}$$

for $K \neq 0$, and

$$\langle 0|H_r|2\rangle = \langle 2|H_r|0\rangle = 2^{-3/2}(B-A)\left[N(N-1)(N+1)(N+2)\right]^{1/2} \tag{7.4}$$

for $K = 0$ and $\tau = 1$.

They obey the selection rules

$$\Delta\lambda \equiv \lambda - \lambda' = 0, \quad \Delta\tau = \Delta N = 0, \quad \Delta K = 0, \pm 2. \tag{8}$$

### 2.2. Spin-Rotational States in $T_1$

For a symmetric top with spin, three sets of commuting operators can be formed (see Appendix in Ref. [1] for commutation rules involving all relevant momenta and their projections on the MCF and LCF axes). The first set is obtained by adding $\mathbf{S}^2$ and $S_{\tilde{z}}$ to the above rotational angular momenta. The EVR wavefunctions $|\Gamma_T; NK\tilde{K}\rangle$ ($\Gamma_T = B_{1u}$ for the $T_1$ state vibrationless wavefunction $|\Gamma_T\rangle$) are multiplied by the spin functions $|S\tilde{\sigma}\rangle$, where $S$ is the total spin quantum number and $\tilde{\sigma}$ is an eigenvalue of $S_{\tilde{z}}$. We shall call this Representation I, the uncoupled-spin representation in the LCF. The second set includes the operators $\mathbf{S}^2$, $\mathbf{J}^2$, $J_z$, $J_{\tilde{z}}$, and $S_z$. The rotational part of their common eigenfunctions is $|JP\tilde{P}\rangle$ and the spin part is $|S\sigma\rangle$. Here, $J$ is the total angular momentum quantum number and $P, \tilde{P}$, and

$\sigma$ are eigenvalues of $J_z$, $J_{\tilde{z}}$, and $S_z$, respectively. This is Representation II, the uncoupled-spin representation in the MCF. The third set of commuting operators is $\mathbf{S}^2$, $\mathbf{J}^2$, $\mathbf{N}^2$, $N_z$, and $J_{\tilde{z}}$, and the corresponding mixed spin-rotational wavefunctions are $|SJNK\tilde{P}\rangle$. This is Representation III, the coupled-spin representation. This notation also will be used for the singlet-state rotational wavefunction, in which case one has

$$|SJNK\tilde{P}\rangle = \delta_{S0}\delta_{JN}\delta_{\tilde{P}\tilde{K}}|NK\tilde{K}\rangle. \tag{9}$$

Then the symmetrized function (3) is denoted as

$$|\Gamma_r\lambda\tau SJNK\tilde{P}\rangle = f_K 2^{-1/2}\left[|SJNK\tilde{P}\rangle + \tau|SJN,-K,\tilde{P}\rangle\right] \tag{10}$$

for $K \geq 0$ and $\tau = \pm 1$, and the expansion (6) for the ground state takes the form

$$|\Gamma_S\Gamma_r''\lambda''\tau''S''J''N''i''\tilde{P}''\rangle = \sum_{K''} C_{K''}^{(\Gamma_S\Gamma_r''\lambda''\tau''S''J''N''i'')}|\Gamma_r''\lambda''\tau''S''J''N''K''\tilde{P}''\rangle, \tag{11}$$

where the ground state quantities are double-primed.

The spin-rotational functions can be expanded in terms of products of the pure rotational and spin functions using both uncoupled Representations I and II. According to the momentum-addition rule [37], which for Representations I and II is written as $\mathbf{J} = \mathbf{N} + \mathbf{S}$ and $\mathbf{N} = (-\mathbf{S}) + \mathbf{J}$, respectively, the expansions have the form [1,45]

$$|SJNK\tilde{P}\rangle = (-1)^{N-S+\tilde{P}}\sqrt{2J+1}\sum_{\tilde{K}\tilde{\sigma}}\begin{pmatrix} N & S & J \\ \tilde{K} & \tilde{\sigma} & -\tilde{P}\end{pmatrix}|NK\tilde{K};S\tilde{\sigma}\rangle, \tag{12}$$

$$|SJNK\tilde{P}\rangle = (-1)^{S-J+K}\sqrt{2N+1}\sum_{P\sigma}\begin{pmatrix} S & J & N \\ \sigma & P & -K\end{pmatrix}|JP\tilde{P}\rangle\theta|S\sigma\rangle, \tag{13}$$

where $\theta$ is the time-reversal operator [37],

$$\theta|S\sigma\rangle = (-1)^{S-\sigma}|S,-\sigma\rangle. \tag{14}$$

With the use of Eq. (14) the expansion in Eq. (13) can be recast as

$$|SJNK\tilde{P}\rangle = \sqrt{2N+1}\sum_{P\sigma}(-1)^{J+P}\begin{pmatrix} J & S & N \\ -P & \sigma & K\end{pmatrix}|JP\tilde{P};S\sigma\rangle, \tag{15}$$

where (...) denotes a Wigner 3-$J$ symbol.

We will use the symmetrized spin-rotational wavefunctions in the form of Eq. (10) as the basis set for an asymmetric rotor with the spin-spin coupling. Again, the rotational Hamiltonian (1) conserves all the quantum numbers except for $K$. Its nonvanishing matrix elements in the symmetrized basis (10) calculated with the use of expansion (12) are

$$\langle\Gamma_r\lambda\tau SJNK\tilde{P}|H_r|\Gamma_r\lambda\tau SJNK'\tilde{P}\rangle \equiv \langle K|H_r|K'\rangle,$$

where $\langle K|H_r|K'\rangle$ is given by (7). The selection rules are the same as in Eq. (8) plus $\Delta J = 0$.

### 2.3. Fine Structure of the Spin-Rotational States in $T_1$

The Hamiltonian of the spin-spin interaction in the triplet state has the form [43]

$$H_{SS} = D\left(S_x^2 - \frac{1}{3}\mathbf{S}^2\right) + E\left(S_z^2 - S_y^2\right), \tag{16}$$

where $S_{x,y,z}$ are projections of the spin angular momentum operator on the MCF axes, and $D$ and $E$ are the fine structure splitting constants given in Table 2. In the nonrotating molecule $H_{SS}$ has three eigenfunctions,

$$H_{SS}|T_{x,y,z}\rangle = T_{x,y,z}|T_{x,y,z}\rangle, \tag{17}$$

where

$$T_z = -\frac{2}{3}D, \quad T_y = \frac{1}{3}D + E, \quad T_z = \frac{1}{3}D - E. \tag{18}$$

The eigenfunctions obey the relationships

$$S_x|T_x\rangle = S_y|T_y\rangle = S_z|T_z\rangle = 0. \tag{19}$$

These functions transform as the $x, y, z$ components of a vector under the $D_2$ group rotations of the electronic spin variables according to $\Gamma_\sigma = B_3, B_2$, and $B_1$, respectively. Since these rotations change only the sign of $S_x$, $S_y$, and $S_z$, the Hamiltonian (16) is invariant and, hence, has no off-diagonal matrix elements. Similarly, the products in Eq. (19) transform by $\Gamma_\sigma \times \Gamma_\sigma = A$ and, hence, identically vanish. Thus, Eqs. (18) and (19) are consequences of the symmetry properties of the system.

The above wavefunctions can also be expressed in terms of the spin functions $|S\sigma\rangle$ with a definite spin projection $\sigma$ [38],

$$\begin{aligned} |T_x\rangle &= -i2^{-1/2}\left(|11\rangle - |1,-1\rangle\right), \\ |T_y\rangle &= 2^{-1/2}\left(|11\rangle + |1,-1\rangle\right), \\ |T_z\rangle &= -i|10\rangle. \end{aligned} \tag{20}$$

Let us define Cartesian components of two tensors with zero traces,

$$T_{ij} = \frac{1}{2}(S_iS_j + S_jS_i) - \frac{1}{3}\mathbf{S}^2\delta_{ij},$$

$$Q_{ij} = Q_{ii}\delta_{ij}, \quad Q_{xx} = \frac{2}{3}D, \quad Q_{yy} = -\frac{1}{3}D - E, \quad Q_{zz} = -\frac{1}{3}D + E, \tag{21}$$

and the corresponding spherical tensors $T_\nu^{(k)}$ and $Q_\nu^{(k)}$ of the second rank $k = 2$ [37] by

$$T_0^{(2)} = -\sqrt{\frac{3}{2}}T_{zz}, \quad T_{\pm1}^{(2)} = \pm(T_{xz} \pm iT_{yz}), \quad T_{\pm2}^{(2)} = -\frac{1}{2}(T_{xx} - T_{yy} \pm 2iT_{xy}),$$

$$Q_0^{(2)} = 6^{-1/2}(D - 3E), \quad Q_{\pm1}^{(2)} = 0, \quad Q_{\pm2}^{(2)} = -\frac{1}{2}(D + E), \tag{22}$$

with all projections in Eqs. (21) and (22) being taken on the MCF axes. Then Eq. (16) takes the form

$$H_{SS} = \sum_{\nu=-k}^{k} (-1)^{k-\nu} Q_{\nu}^{(k)} T_{-\nu}^{(k)}, \tag{23}$$

which enables us to invoke the Wigner–Eckart theorem to calculate the relevant matrix elements for a rotating molecule.

Consider first the matrix elements of $H_{SS}$ in the nonsymmetrized basis $|SJNK\tilde{P}\rangle$. Since $H_{SS}$ commutes with $\mathbf{S}^2$, $\mathbf{J}^2$, and $J_z$, and does not commute with $\mathbf{N}^2$ and $N_z$, it is diagonal in $S$, $J$, and $\tilde{P}$ and off-diagonal in $N$ and $K$. Introducing the notation

$$\langle SJNK\tilde{P}|H_{SS}|S'J'N'K'\tilde{P}'\rangle \equiv \delta_{SS}\delta_{JJ'}\delta_{\tilde{P}\tilde{P}'}\langle NK|H_{SS}|N'K'\rangle$$

and inserting expansion (15), we obtain

$$\langle NK|H_{SS}|N'K'\rangle \equiv \langle N'K'|H_{SS}|NK\rangle = \sqrt{(2N+1)(2N'+1)} \times$$
$$\times \sum_{\nu P\sigma\sigma'} (-1)^{2-\nu} Q_{\nu}^{(2)} \begin{pmatrix} J & S & N \\ -P & \sigma & K \end{pmatrix} \begin{pmatrix} J & S & N' \\ -P & \sigma' & K' \end{pmatrix} \langle S\sigma|T_{-\nu}^{(2)}|S\sigma'\rangle. \tag{24}$$

The advantage of using expansion (15) rather than (12) is that both $Q_{\nu}^{(2)}$ and $\langle S\sigma|T_{-\nu}^{(2)}|S\sigma'\rangle$ are independent of Euler angles, so that the rotational factor is merely $\delta_{JJ'}\delta_{PP'}\delta_{\tilde{P}\tilde{P}'}$. The remaining pure spin matrix element in Eq. (24) is calculated by applying the Wigner–Eckart theorem [37],

$$\langle S\sigma|T_{-\nu}^{(2)}|S\sigma'\rangle = (-1)^{S-\sigma-1} \begin{pmatrix} S & 2 & S \\ -\sigma & -\nu & \sigma' \end{pmatrix} \langle S||T^{(2)}||S\rangle, \tag{25}$$

where the reduced matrix element is

$$\langle S||T^{(2)}||S\rangle = \frac{1}{2\sqrt{6}} [(2S-1)2S(2S+1)(2S+2)(2S+3)]^{1/2} \tag{26}$$

($= \sqrt{5}$ for $S = 1$). Substituting Eqs. (25) and (26) into Eq. (24) and performing summations, we obtain for $S = 1$

$$\langle NK|H_{SS}|N'K'\rangle \equiv \langle N'K'|H_{SS}|NK\rangle = (-1)^{J-K}\sqrt{5(2N+1)(2N'+1)} \times$$
$$\times \begin{pmatrix} 2 & N' & N \\ K'-K & -K' & K \end{pmatrix} \begin{Bmatrix} N & N' & 2 \\ 1 & 1 & J \end{Bmatrix} Q_{K-K'}^{(2)}, \tag{27}$$

where $\{\ldots\}$ stands for a Wigner $6-J$ symbol. The following selection rules stem from Eqs. (22) and (27):

$$\Delta S = \Delta J = 0, \quad \Delta N = 0, \pm 1, \pm 2, \quad \Delta K = 0, \pm 2. \tag{28}$$

Matrix elements (27) also obey the relation

$$\langle N, -K|H_{SS}|N', -K'\rangle \equiv (-1)^{N+N'}\langle NK|H_{SS}|N'K'\rangle, \tag{29}$$

which is easy to deduce from the symmetry properties of the $3-J$ symbol [37].

The matrix elements in the symmetrized basis (10) are off-diagonal in $\tau$, $N$, and $K$. Introducing the notation

$$\langle \Gamma_r \lambda \tau S J N K \tilde{P} | H_{SS} | \Gamma_r \lambda' \tau' S' J' N' K' \tilde{P}' \rangle \equiv \delta_{\lambda\lambda'} \delta_{SS'} \delta_{JJ'} \delta_{\tilde{P}\tilde{P}'} \langle \tau N K | H_{SS} | \tau' N' K' \rangle \quad (30)$$

and applying (29), we find

$$\langle \tau N K | H_{SS} | \tau' N' K' \rangle = f_K f_{K'} \left[ \langle N K | H_{SS} | N' K' \rangle + \tau \langle N, -K | H_{SS} | N' K' \rangle \right].$$

It is easy to verify that the $H_{SS}$ matrix is symmetric in this basis, as well as in the original basis (see Eq. (24)). As is evident from Eq. (30), the following selection rule, in addition to (28), applies for the spin-spin coupling:

$$\Delta\lambda \equiv \lambda - \lambda' = 0. \quad (31)$$

Let us write down explicitly the nonvanishing matrix elements of $H_{SS}$ in terms of the matrix elements (27),

$$\begin{aligned} &\langle 1N0 | H_{SS} | \tau' N' 2 \rangle = \sqrt{2} \langle N0 | H_{SS} | N' 2 \rangle, \\ &\langle \tau N 1 | H_{SS} | \tau' N' 1 \rangle = \langle N1 | H_{SS} | N' 1 \rangle + \tau \langle N, -1 | H_{SS} | N' 1 \rangle, \\ &\langle \tau N K | H_{SS} | \tau' N' K' \rangle = \langle N K | H_{SS} | N' K' \rangle, \quad K + K' \neq 2. \end{aligned} \quad (32)$$

The total Hamiltonian for the triplet state is written as

$$H_T = H_r + \varepsilon H_{SS}, \quad (33)$$

where $\varepsilon$ is a parameter to be used for drawing a correlation diagram. Since $H_T$ has no matrix elements between the symmetrized basis states (10) differing in either $\Gamma_r$ or $\lambda$, its eigenfunctions can also be characterized by $\Gamma_r$ and $\lambda$ (in addition to the conserving quantum numbers $S$, $J$, and $\tilde{P}$). Putting a prime on all quantities relating to the triplet state, we obtain the following representation for the wavefunctions:

$$|\Gamma_T \Gamma_r' \lambda' S' J' i' \tilde{P}' \rangle = \sum_{\tau' N' K'} C_{\tau' N' K'}^{(\Gamma_T \Gamma_r' \lambda' S' J' i')} |\Gamma_r' \lambda' \tau' S' J' N' K' \tilde{P}' \rangle, \quad (34)$$

where $i'$ labels the eigenvalues of $H_T$ for a given $\Gamma_r'$, $\lambda'$, $S'$, $J'$. For any given $J'$, $\Gamma_r'$ runs over the IR's of the $D_2$ group, and, for each $\Gamma_r'$, the $\lambda'$ assumes a definite value from Table 3. The summation in the right-hand side of Eq. (34) is taken over $N' = J'$, $J' \pm 1$; $K'$ runs from 0 to $N'$ over even or odd values for a given $\Gamma_r'$, according to Table 3; and the sum over $\tau'$ involves only a single term since $\tau'$ is uniquely fixed by $\lambda'$ and $N'$ according to the definition in Eq. (5).

### 2.4. Singlet Contamination of the Triplet State

The triplet state is assumed to be mixed, *via* spin-orbit coupling, with an excited singlet state $S_n$ having $\Gamma_{S_n} = B_{2u}$ symmetry [26, 31], giving it radiative character. (We do not consider a mixing of the ground state with an excited triplet state $T_n$, which may be of importance in pyrazine [46].) The intensities in the $T_1 \leftarrow S_0$ absorption spectra depend on the degree of this mixing. We first consider the general restrictions, due to the Pauli principle, on the symmetry

species of the levels that can mix with each other. These restrictions are independent of the form of the particular mixing operator.

Let $\psi$ and $\psi'$ stand for the total wavefunctions of the states that are coupled *via* some interaction Hamiltonian $H_{int}$. They are represented as products of the electronic, vibrational, rotational, and nuclear-spin wavefunctions,

$$\psi = \psi_e\psi_v\psi_r\psi_{ns}, \quad \psi' = \psi'_e\psi'_v\psi'_r\psi'_{ns},$$

whose symmetry properties depend on their behavior with respect to the feasible permutations [47] of the nuclei. Every such permutation $P$ can be performed by a rotation $R \in D_2$. This is done in three steps. First, the MCF is rotated with respect to the LCF, which results in the transformation $\psi_r \to \Gamma_r\psi_r$, where $\Gamma_r$ is an IR of $D_2$. Second, the electronic coordinates and nuclear displacements must be returned to their initial values by the backward rotation $R^{-1}$; in $D_2$, it is the same as $R$. This leads to $\psi_e\psi_v \to (\Gamma_e\psi_e)(\Gamma_v\psi_v)$, where $\Gamma_e$ and $\Gamma_v$ are again IR's of $D_2$. Third, the permutation $P$ is applied to the nuclear spin variables resulting in $\psi_{ns} \to \Gamma_{ns}\psi_{ns}$. Since the set of three feasible permutations plus the unit (no rotation) operator constitute a group isomorphous to $D_2$, $\Gamma_{ns}$ is an IR of $D_2$ as well.

The symmetry species of the total wavefunction with respect to the feasible permutations is therefore the product of the symmetry species of each of the components,

$$\Gamma = \Gamma_e\Gamma_v\Gamma_r\Gamma_{ns}, \quad \Gamma' = \Gamma'_e\Gamma'_v\Gamma'_r\Gamma'_{ns}. \tag{35}$$

These permutations involve spinless carbon nuclei, spin one nitrogen nuclei and an even number (two or four) of protons whose total spin is again an integer. Then, according to the Pauli principle, the total wavefunction must be invariant under the feasible permutations of the nuclei; i.e.,

$$\Gamma = \Gamma' = A, \tag{36}$$

where $A$ is the totally symmetric representation of $D_2$. Now, the interaction Hamiltonian $H_{int}$ of interest is independent of nuclear spin. This means that $\psi_{ns} = \psi'_{ns}$ and $\Gamma_{ns} = \Gamma'_{ns}$. Combining this with Eqs. (35) and (36) gives the final relation

$$\Gamma_e\Gamma_v\Gamma_r = \Gamma'_e\Gamma'_v\Gamma'_r = \Gamma_{ns}. \tag{37}$$

For the mixing of the vibrationless $S_n$ and $T_1$ states one has $\Gamma_e = B_{2u}$, $\Gamma'_e = B_{1u}$, and $\Gamma_v = \Gamma'_v = A_g$. Then Eq. (37) reduces to $B_2\Gamma_r = B_1\Gamma'_r = \Gamma_{ns}$, where the $D_2$ group IR's are used instead of $D_{2h}$. Table 4 shows the symmetry species of the rotational levels that are allowed to mix according to this result.

*Table 4*

**Symmetry species $\Gamma_r$ and $\Gamma_{r'}$ of the rotational sublevels of the vibrationless $B_{1u}$ and $B_{2u}$ states, respectively, that will mix *via* an arbitrary coupling independent of nuclear spin. The symmetry species of the corresponding nuclear spin wavefunctions, $\Gamma_{ns}$, are also given**

| $\Gamma_r$ | $\Gamma'_r$ | $\Gamma_{ns}$ |
|---|---|---|
| $A$ | $B_3$ | $B_1$ |
| $B_1$ | $B_2$ | $A$ |
| $B_2$ | $B_1$ | $B_3$ |
| $B_3$ | $A$ | $B_2$ |

Next, we derive an expression for matrix elements of the spin-orbit Hamiltonian $H_{so}$, which couples $T_1$ to the singlet manifold $S_n$. In the Hartree–Fock self-consistent-field approximation $H_{so}$ is represented by a sum of one-electron operators, each acting on the coordinates of a single electron [1, 34],

$$H_{so} = \sum_a \mathbf{b}_a \mathbf{s}_a, \tag{38}$$

where $\mathbf{b}_a$ is a body-fixed vector, whose components in the MCF depend on the Cartesian coordinates of the $a$-th electron and on the nuclear displacements, and $\mathbf{s}_a$ is the spin operator of the $a$-th electron. Equation (38) can be further simplified providing that the electronic states of interest are the ground state and only one-electron excited states. For instance, the $^1B_{2u}$ and $^3B_{1u}$ states of pyrazine are formed by promoting a single electron from the filled $\pi_2$ and $n_+$ orbitals, respectively, to the empty orbital $\pi_4^*$ [31, 48]. Then the summation in Eq. (38) can be taken over two electrons,

$$H_{so} = \mathbf{b}_1 \mathbf{s}_1 + \mathbf{b}_2 \mathbf{s}_2. \tag{39}$$

The equivalence of Eqs. (38) and (39) can be proved by a straightforward calculation; e.g., using the method of secondary quantization [37].

In order to calculate the $S_n - T_1$ vibronic matrix element of $H_{so}$, Eq. (39), we note that the spatial part of the electronic wavefunction is symmetric with respect to the electrons' permutation for the singlet state and antisymmetric for the triplet state. Then, the vector

$$\mathbf{c} \equiv \langle \Gamma_{S_n} | \mathbf{b}_1 | \Gamma_T \rangle = -\langle \Gamma_{S_n} | \mathbf{b}_2 | \Gamma_T \rangle \tag{40}$$

can be defined for each participating singlet state, and the desired matrix element takes the form

$$\langle \Gamma_{S_n} | H_{so} | \Gamma_T \rangle = \mathbf{cG} = \sum_{\sigma=0,\pm1} (-1)^{1-\sigma} c_\sigma^{(1)} G_{-\sigma}^{(1)}, \tag{41}$$

where $\mathbf{G} = \mathbf{s}_1 - \mathbf{s}_2$. The components of the first-rank spherical tensors are defined as [37]

$$c_0^{(1)} = ic_z, \quad c_{\pm1}^{(1)} = \mp i 2^{-1/2} (c_x \pm i c_y), \tag{42}$$

and similarly for $G_\sigma^{(1)}$. The matrix elements of $G_\sigma^{(1)}$ over the spin functions $|S\sigma\rangle$ are easily calculated to give

$$\langle 00 | (-1)^{1-\sigma} G_{-\sigma}^{(1)} | 1\sigma' \rangle = -i\delta_{\sigma\sigma'}. \tag{43}$$

In the particular case of pyrazine the spatial parts of the electronic wavefunctions may be written in terms of one-electron orbitals as

$$|\Gamma_{S_n}\rangle = 2^{-1/2} \left[ \pi_2(\mathbf{r}_1)\pi_4^*(\mathbf{r}_2) + \pi_2(\mathbf{r}_2)\pi_4^*(\mathbf{r}_1) \right],$$
$$|\Gamma_T\rangle = 2^{-1/2} \left[ n_+(\mathbf{r}_1)\pi_4^*(\mathbf{r}_2) - n_+(\mathbf{r}_2)\pi_4^*(\mathbf{r}_1) \right],$$

where $\mathbf{r}_{1,2}$ are the coordinates of the two electrons. Then,

$$\mathbf{c} = \frac{1}{2} \langle \pi_2 | \mathbf{b} | n_+ \rangle.$$

Since $\pi_2$ and $n_+$ transform as $B_3$ and $A$, respectively, the vector $\mathbf{c}$ has only one nonvanishing component,

$$c_x = \frac{1}{2}\langle \pi_2 | b_x | n_+ \rangle \equiv v_{so}\sqrt{2}, \quad c_y = c_z = 0, \tag{44}$$

where the spin-orbit coupling parameter, $v_{so}$, is introduced. Using Eq. (44), we recast Eq. (42) as

$$c_\sigma^{(1)} = -i\sigma v_{so}. \tag{45}$$

From Eqs. (20), (43), and (45) we deduce that only the $T_x$ triplet sublevel is contaminated with the $S_n$ singlet *via* spin-orbit coupling (41). This result is a consequence of symmetry [38]. Indeed, $H_{so}$ is invariant under the $D_2$ group transformations of the electronic space and spin coordinates and nuclear displacements. Hence, a vibrationless triplet level $|\Gamma_T \Gamma_\sigma\rangle$ can be mixed with a vibrationless singlet $|\Gamma_{S_n}\rangle$ only when $\Gamma_T \times \Gamma_\sigma = \Gamma_{S_n}$. For $\Gamma_T = B_1$ and $\Gamma_{S_n} = B_2$, it follows that only the $T_x$ level which has $\Gamma_\sigma = B_3$ mixes with the singlet.

Next, we calculate the spin-rotational matrix elements of Eq. (41),

$$\langle SJNK\tilde{P}|H_{so}|S'J'N'K'\tilde{P}'\rangle \equiv \delta_{JN}\delta_{JJ'}\delta_{\tilde{P}\tilde{P}'}\langle K|H_{so}|J'N'K'\rangle, \tag{46}$$

where $S = 0$ and $S' = 1$. Now $H_{so}$ stands for $\langle \Gamma_{S_n}|H_{so}|\Gamma_T\rangle$, and common notations are used for the singlet and triplet wavefunctions (see Eq. (9)). Inserting Eq. (41) and the spin-rotational functions in the form of expansion (15), we obtain after simple algebra [1]

$$\langle K|H_{so}|J'N'K'\rangle = v_{so}(-1)^{J'-K+1}\sqrt{2N'+1}\sum_{\sigma'=\pm 1}\sigma' \begin{pmatrix} J' & 1 & N' \\ -K & \sigma' & K' \end{pmatrix}, \tag{47}$$

where use was made of Eqs. (43) and (45). These matrix elements have the following obvious property:

$$\langle -K|H_{so}|J'N', -K'\rangle \equiv (-1)^{N+N'}\langle K|H_{so}|J'N'K'\rangle, \tag{48}$$

where $N = J'$ according to Eq. (46). The matrix elements of $H_{so}$ in the symmetrized basis (10),

$$\langle \Gamma_r \lambda \tau SJNK\tilde{P}|H_{so}|\Gamma_r' \lambda' \tau' S'J'N'K'\tilde{P}'\rangle \equiv \delta_{\lambda\lambda'}\delta_{JN}\delta_{JJ'}\delta_{\tilde{P}\tilde{P}'}\langle \tau K|H_{so}|\tau' J'N'K'\rangle, \tag{49}$$

can be expressed in terms of (47) as follows:

$$\langle \tau K|H_{so}|\tau' J'N'K'\rangle = f_K f_{K'}\left[\langle K|H_{so}|J'N'K'\rangle + \tau'\langle K|H_{so}|J'N', -K'\rangle\right], \tag{50}$$

where use was made of Eq. (48). The selection rules for the matrix elements (49) are

$$\Delta\lambda = 0, \quad \Delta S = \pm 1, \quad \Delta J = 0, \quad \Delta N = 0, \pm 1, \quad \Delta K = \pm 1. \tag{51}$$

It is seen that $H_{so}$ conserves $\lambda$ and changes $K$ by one. According to Table 3 it means that $H_{so}$ mixes the states of the following rotational symmetries $\Gamma_r$: $B_1 \leftrightarrow B_2$ and $B_3 \leftrightarrow A$. In other words, $H_{so}$ obeys the general requirements for a mixing operator as displayed in Table 4. Substituting Eq. (47) into (50), we obtain

$$\langle \tau K|H_{so}|\tau' J'N'K'\rangle = v_{so} f_K f_{K'} (-1)^{J'-K+1}\sqrt{2N'+1}\times$$
$$\times \sum_{\sigma'=\pm 1} \sigma' \left[ \begin{pmatrix} J' & 1 & N' \\ -K & \sigma' & K' \end{pmatrix} + \tau' \begin{pmatrix} J' & 1 & N' \\ -K & \sigma' & -K' \end{pmatrix} \right]. \qquad (52)$$

Penner et al. [25] introduced the conjecture of a so-called $M_{J'}$ selectivity of the spin-orbit coupling, assuming that, out of a manifold of triplet states with a given $J'$, a single state with $M_{J'} = 0$ borrows oscillator strength from an excited singlet. This is shown to be incorrect by our Eq. (52). It is easy to verify that, for every $J' \geq 1$, all $3(2J'+1)$ triplet sublevels borrow oscillator strength from $S_n$.

The next step is to calculate the singlet-contaminated triplet wavefunction,

$$|\Gamma_T; \Gamma'_\tau \lambda' \tau' S' J' N' K' \tilde{P}'\rangle \rightarrow$$
$$\rightarrow \sum \frac{\langle \Gamma_\tau \lambda \tau S J N K \tilde{P}|H_{so}|\Gamma'_\tau \lambda' \tau' S' J' N' K' \tilde{P}'\rangle}{E_T - E_{S_n}} |\Gamma_{S_n}; \Gamma_\tau \lambda \tau S J N K \tilde{P}\rangle, \qquad (53)$$

where the unperturbed triplet function is omitted and the sum is taken over all quantum numbers of the $S_n$ state. The energy denominator depends on the quantum numbers of the participating states, and in general Eq. (53) depends on the rotational constants of the contaminating singlet state. However, in case of pyrazine the $S_n$ state is assumed to lie at much higher energy than the $T_1$ state, in which case the purely electronic energy gap $\Delta E$ between $S_n$ and $T_1$ can be substituted for the energy denominator in Eq. (53). We also note that, strictly speaking, the linear combinations (34) found after diagonalizing the total triplet state Hamiltonian (33) rather than the basis functions (10) should be corrected for the contamination with $S_n$. However, after making the above approximation to the energy denominator, we obtain the same result by calculating (53) and inserting it into (34). Finally, the symmetric top wavefunctions for the $S_n$ state are used in Eq. (53), thus neglecting the $S_n$ asymmetry effect. As a result, the mixing of the triplet state is independent of the rotational constants of the contaminating singlet state.

Inserting Eqs. (49) and (52) into (53) gives

$$|\Gamma_T; \Gamma'_\tau \lambda' \tau' S' J' N' K' \tilde{P}'\rangle \rightarrow \frac{1}{\Delta E} \sum \delta_{\lambda\lambda'} \delta_{JN} \delta_{JJ'} \delta_{\tilde{P}\tilde{P}'} \langle \tau K|H_{so}|\tau' J' N' K'\rangle \times$$
$$\times |\Gamma_{S_n}; \Gamma_\tau \lambda \tau S J N K \tilde{P}\rangle = \frac{v_{so}}{\Delta E} \sum_{P'=0}^{J'} f_{P'} f_{K'} (-1)^{J'-P'+1} \sqrt{2N'+1} \times$$
$$\times \sum_{\sigma'=\pm 1} \sigma' \left[ \begin{pmatrix} J' & 1 & N' \\ -P' & \sigma' & K' \end{pmatrix} + \tau' \begin{pmatrix} J' & 1 & N' \\ -P' & \sigma' & -K' \end{pmatrix} \right] |\Gamma_{S_n}; \Gamma_\tau \lambda' \tau S J' J' P' \tilde{P}'\rangle, \qquad (54)$$

where we changed the notation $K$ to $P'$ following the convention that $K$ is a projection of $\mathbf{N}$ and $P$ is a projection of $\mathbf{J}$. In the singlet function, $\tau$ is fixed by the condition that $\lambda = \lambda'$, which gives (see the definition of $\lambda$ in Eq. (5))

$$\tau = \tau'(-1)^{J'+N'}. \qquad (55)$$

Equation (54) can be derived in a different way. First, we calculate the contaminated triplet spin wavefunction neglecting rotations and using Eqs. (41), (43), and (45),

$$|\Gamma_T; S'\sigma'\rangle \rightarrow \frac{1}{\Delta E} \langle \Gamma_{S_n}; 00|H_{so}|\Gamma_T; S'\sigma'\rangle |\Gamma_{S_n}; 00\rangle = -\frac{v_{so}}{\Delta E} \sigma' |\Gamma_{S_n}; 00\rangle. \qquad (56)$$

Then, we insert this into expansions (10) and (15) for the symmetrized spin-rotational function,

$$|\Gamma_T;\Gamma_r'\lambda'\tau'S'J'N'K'\tilde{P}'\rangle \to -\frac{v_{so}}{\Delta E} f_{K'} 2^{-1/2}\sqrt{2N'+1} \sum_{P'=-J'}^{J'} (-1)^{J'+P'} \times$$
$$\times \sum_{\sigma'=\pm 1} \sigma' \left[ \begin{pmatrix} J' & 1 & N' \\ -P' & \sigma' & K' \end{pmatrix} + \tau' \begin{pmatrix} J' & 1 & N' \\ -P' & \sigma' & -K' \end{pmatrix} \right] |\Gamma_{S_n}; J'P'\tilde{P}'; 00\rangle. \quad (57)$$

Here, the singlet wavefunction has also to be symmetrized. We rename the summation variables, $P' \to K$ and $\sigma' \to \sigma$, and recast the sum over $K$ as

$$\sum_{K=0}^{J'} f_K^2 (-1)^{J'+K} \sum_{\sigma=\pm 1} \sigma \left[ \begin{pmatrix} J' & 1 & N' \\ -K & \sigma & K' \end{pmatrix} + \tau' \begin{pmatrix} J' & 1 & N' \\ -K & \sigma & -K' \end{pmatrix} \right] |\Gamma_{S_n}; J'K\tilde{P}'; 00\rangle +$$
$$+ \sum_{K=0}^{J'} f_K^2 (-1)^{J'-K} \sum_{\sigma=\pm 1} \sigma \left[ \begin{pmatrix} J' & 1 & N' \\ K & \sigma & K' \end{pmatrix} + \tau' \begin{pmatrix} J' & 1 & N' \\ K & \sigma & -K' \end{pmatrix} \right] |\Gamma_{S_n}; J', -K, \tilde{P}'; 00\rangle. \quad (58)$$

In the second term of Eq. (58) we change the sign of the summation variable, $\sigma \to -\sigma$. Using the symmetry properties of the 3-$J$ symbols [37] and the identity $(\tau')^2 = 1$, we rewrite Eq. (58) in the form

$$\sum_{K=0}^{J'} f_K^2 (-1)^{J'+K} \sum_{\sigma=\pm 1} \sigma \left[ \begin{pmatrix} J' & 1 & N' \\ -K & \sigma & K' \end{pmatrix} + \tau' \begin{pmatrix} J' & 1 & N' \\ -K & \sigma & -K' \end{pmatrix} \right] \times$$
$$\times \left[ |J'K\tilde{P}'\rangle + \tau |J', -K, \tilde{P}'\rangle \right] |\Gamma_{S_n}; 00\rangle, \quad (59)$$

where $\tau$ is given by Eq. (55). By definitions (3)–(5), (9), and (10), the total wavefunction in Eq. (59) can be written as

$$2^{1/2} f_K^{-1} |\Gamma_{S_n}; \Gamma_r \lambda \tau S J' J' K \tilde{P}'; 00\rangle \quad (60)$$

with $\lambda \equiv \tau(-1)^{J'} = \tau'(-1)^{N'} = \lambda'$. Then inserting Eqs. (58)–(60) into (57) again leads to Eq. (54).

### 2.5. Intensities of Individual Singlet-Triplet Transitions

The contamination of the triplet state with the singlet state $S_n$ results in a nonzero transition moment $\langle \Gamma_S | \mu | \Gamma_T \Gamma_\sigma \rangle$, which is proportional to $\langle \Gamma_S | \mu | \Gamma_{S_n} \rangle$, where $\mu$ is the electric dipole moment operator. The only nonvanishing component of the transition moment in the MCF for $\Gamma_S = A_{1g}$ and $\Gamma_{S_n} = B_{2u}$ is $\langle \Gamma_S | \mu_y | \Gamma_{S_n} \rangle$ since the symmetry species of $\mu_y$ is $B_{2u}$. The corresponding Hougen's intensity parameter $\mu(B_{3g})$ [38] can be introduced by the relationship

$$\mu(B_{3g}) = \sqrt{2} \frac{v_{so}}{\Delta E} \langle \Gamma_S | \mu_y | \Gamma_{S_n} \rangle \equiv \frac{c_x \mu_y}{\Delta E}, \quad (61)$$

where $\mu_y$ now stands for the matrix element and the notation $\mu(B_{3g})$ reflects the fact that the triplet sublevel $T_x$ borrowing the $B_{2u} \leftarrow A_{1g}$ oscillator strength belongs to the symmetry species $\Gamma_\sigma = B_{3g}$.

The intensity of an individual transition is given by

$$I(\Gamma_T\Gamma'_\tau\lambda' S' J' i' \leftarrow \Gamma_S\Gamma''_\tau\lambda''\tau'' S'' J'' N'' i'') =$$
$$= 3\sum_{\tilde{P}'\tilde{P}''}\left|\langle\Gamma_T;\Gamma'_\tau\lambda' S' J' i'\tilde{P}'|\boldsymbol{\mu}\mathbf{e}|\Gamma_S;\Gamma''_\tau\lambda''\tau'' S'' J'' N'' i''\tilde{P}''\rangle\right|^2, \tag{62}$$

where $\mathbf{e}$ is a unit vector in the direction of the electric field. Defining the first-rank spherical tensor components of $\boldsymbol{\mu}$ and $\mathbf{e}$ both in the LCF and MCF by the relations given in Eq. (42), e.g.,

$$e^{(1)}_{\tilde{0}} = ie_{\tilde{z}}, \quad e^{(1)}_{\pm\tilde{1}} = \mp i2^{-1/2}(e_{\tilde{x}} \pm ie_{\tilde{y}}), \tag{63}$$

and similarly for $\boldsymbol{\mu}$ where tilda indicates the LCF axes, we have

$$\boldsymbol{\mu}\mathbf{e} = \sum_{\tilde{\sigma}=0,\pm1}(-1)^{1-\tilde{\sigma}}\mu^{(1)}_{\tilde{\sigma}}e^{(1)}_{-\tilde{\sigma}}, \tag{64}$$

which is similar to Eq. (41) except that projections are taken in the LCF rather than MCF. The LCF projections are expressed in terms of the MCF projections by [37]

$$\mu^{(1)}_{\tilde{\sigma}} = \sum_{\sigma=0,\pm1}D^{(1)}_{\sigma\tilde{\sigma}}\mu^{(1)}_{\sigma}. \tag{65}$$

In Eqs. (64) and (65), $\mu^{(1)}_\sigma$ and $e^{(1)}_{-\tilde{\sigma}}$ are invariant with respect to rotations whereas the Wigner functions $D^{(1)}_{\sigma\tilde{\sigma}}$ depend on the Euler angles. We substitute Eqs. (64), (65) and expansions (11) and (34) into Eq. (62), obtaining

$$I(\Gamma_T\Gamma'_\tau\lambda' S' J' i' \leftarrow \Gamma_S\Gamma''_\tau\lambda''\tau'' S'' J'' N'' i'') = 3\sum_{\tilde{P}'\tilde{P}''}\left|\sum_{N'K'K''}C^{(i')}_{N'K'}C^{(i'')}_{K''}M_1\right|^2, \tag{66}$$

where we omitted some indices of the coefficients of expansions (11) and (34), and

$$M_1 = \langle\Gamma_T;\Gamma'_\tau\lambda'\tau' S' J' N' K'\tilde{P}'|\sum_{\sigma\tilde{\sigma}}(-1)^{1-\tilde{\sigma}}D^{(1)}_{\sigma\tilde{\sigma}}\mu^{(1)}_\sigma e^{(1)}_{-\tilde{\sigma}}|\Gamma_S;\Gamma''_\tau\lambda''\tau'' S'' J'' N'' K''\tilde{P}''\rangle. \tag{67}$$

The triplet function is approximated by Eq. (54),

$$M_1 = \frac{v_{so}}{\Delta E}\sum_{P'}f_{P'}f_{K'}(-1)^{J'-P'+1}\sqrt{2N'+1}\times$$
$$\times\sum_{\sigma'=\pm1}\sigma'\left[\begin{pmatrix} J' & 1 & N' \\ -P' & \sigma' & K'\end{pmatrix} + \tau'\begin{pmatrix} J' & 1 & N' \\ -P' & \sigma' & -K'\end{pmatrix}\right]M_2, \tag{68}$$

where

$$M_2 = \langle\Gamma_{S_n};\Gamma_\tau\lambda'\tau S J' J' P'\tilde{P}'|\sum_{\sigma\tilde{\sigma}}(-1)^{1-\tilde{\sigma}}D^{(1)}_{\sigma\tilde{\sigma}}\mu^{(1)}_\sigma e^{(1)}_{-\tilde{\sigma}}|\Gamma_S;\Gamma''_\tau\lambda''\tau'' S'' J'' N'' K''\tilde{P}''\rangle \tag{69}$$

and $\tau$ is given by Eq. (55). The electronic factor in Eq. (69) is

$$\langle\Gamma_{S_n}|\mu^{(1)}_\sigma|\Gamma_S\rangle = |\sigma|\mu_y/\sqrt{2}. \tag{70}$$

We will choose the LCF axis $\tilde{z}$ along the electric field since the result is independent of the field direction. Then from Eq. (63) we have $e^{(1)}_{\tilde{0}} = i$, $e^{(1)}_{\pm\tilde{z}} = 0$, and Eq. (69) becomes $M_2 = -i\mu_y M_3/\sqrt{2}$, where

$$M_3 = \langle \Gamma_\tau \lambda' \tau S J' J' P' \tilde{P}' | \sum_{\sigma=\pm 1} D^{(1)}_{\sigma\tilde{0}} | \Gamma''_\tau \lambda'' \tau'' S'' J'' N'' K'' \tilde{P}'' \rangle \tag{71}$$

is the rotational factor. This matrix element is expressed in terms of the integral of a product of three Wigner functions [37]. With the use of Eqs. (9), (10), and (55) the rotational factor becomes

$$\begin{aligned} M_3 &= f_{P'} f_{K''} \delta_{\lambda',-\lambda''} \times \\ &\times \left[ \langle J' K \tilde{P}' | \sum_{\sigma=\pm 1} D^{(1)}_{\sigma\tilde{0}} | J'' K'' \tilde{P}'' \rangle + \tau'' \langle J' K \tilde{P}' | \sum_{\sigma=\pm 1} D^{(1)}_{\sigma\tilde{0}} | J'', -K'', \tilde{P}'' \rangle \right] = \\ &= f_{P'} f_{K''} \delta_{\lambda',-\lambda''} (-1)^{P'-\tilde{P}'} \sqrt{(2J'+1)(2J''+1)} \times \\ &\times \sum_{\sigma=\pm 1} \left[ \begin{pmatrix} J' & 1 & J'' \\ -P' & \sigma & K'' \end{pmatrix} + \tau'' \begin{pmatrix} J' & 1 & J'' \\ -P' & \sigma & -K'' \end{pmatrix} \right] \begin{pmatrix} J' & 1 & J'' \\ -\tilde{P}' & 0 & \tilde{P}'' \end{pmatrix}. \end{aligned} \tag{72}$$

After the insertion of Eqs. (67)–(72) in Eq. (66), the last factor in Eq. (72) squared can be summed to give unity. Thus, we arrive at the final expression for the intensity of an individual transition:

$$\begin{aligned} I(\Gamma_T \Gamma'_\tau \lambda' S' J' i' \leftarrow \Gamma_S \Gamma''_\tau \lambda'' \tau'' S'' J'' N'' i'') &= \frac{1}{4} \delta_{\lambda',-\lambda''} |\mu(B_{3g})|^2 (2J'+1)(2J''+1) \times \\ \times \Bigg| \sum_{N'=|J'-1|}^{J'+1} \sqrt{2N'+1} & \sum_{\substack{K'=0 \\ \text{(only even or odd)}}}^{N'} f_{K'} C^{(i')}_{N'K'} \sum_{\substack{K''=0 \\ \text{(only even or odd)}}}^{J''} f_{K''} C^{(i'')}_{K''} \times \\ \times \sum_{P'=0}^{J'} f^2_{P'} \sum_{\sigma'\sigma=\pm 1} \sigma' F_{P'\sigma'\sigma} \Bigg|^2, \end{aligned} \tag{73}$$

where

$$\begin{aligned} F_{P'\sigma'\sigma} = &\left[ \begin{pmatrix} J' & 1 & N' \\ -P' & \sigma' & K' \end{pmatrix} + \tau' \begin{pmatrix} J' & 1 & N' \\ -P' & \sigma' & -K' \end{pmatrix} \right] \times \\ &\times \left[ \begin{pmatrix} J' & 1 & J'' \\ -P' & \sigma & K'' \end{pmatrix} + \tau'' \begin{pmatrix} J' & 1 & J'' \\ -P' & \sigma & -K'' \end{pmatrix} \right], \end{aligned} \tag{74}$$

and, according to Eq. (5),

$$\tau' = \lambda'(-1)^{N'}, \quad \tau'' = \lambda''(-1)^{J''}. \tag{75}$$

For given $\Gamma'_\tau$ and $\Gamma''_\tau$ the evenness or oddness of $K'$ and $K''$, as well as the values of $\lambda'$ and $\lambda''$, are found from Table 3. The following selection rules are evident from the properties of the Wigner 3-$J$ symbols in Eq. (74):

$$\Delta J = 0, \pm 1, \quad \Delta N = 0, \pm 1, \pm 2, \quad \Delta K = 0, \pm 2. \tag{76}$$

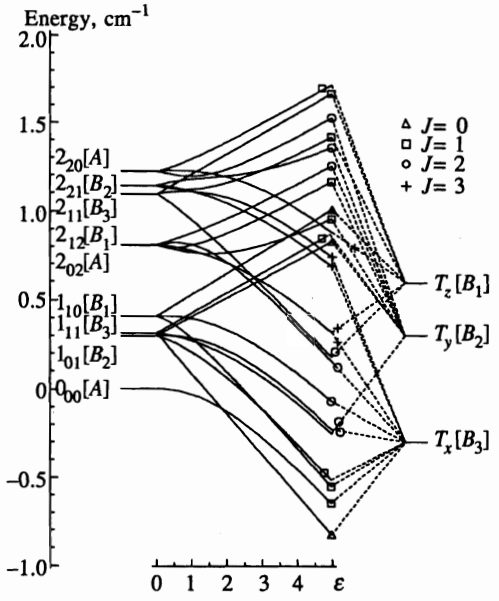


**Fig. 2.** Correlation diagram for the lowest spin-rotational levels of the $T_1$ state of pyrazine in the gas phase

For instance, $P'$ differs from both $K'$ and $K''$ by one, therefore $K'$ and $K''$ differ by 0 or 2. Since the $K$'s are both even or odd, and since the $\lambda$'s are opposite in sign, the allowed transitions are (see Table 3) $A \leftrightarrow B_1$ and $B_2 \leftrightarrow B_3$.

Equation (73) is the main result of the present paper. It may be applied to molecules for which only the spin-spin interaction is important, and in which only one spin sublevel of the nonrotating molecule is radiatively active, as in case of the $T_1 \leftarrow S_0$ absorption spectrum of pyrazine. A more general formula, valid for other molecules, is derived in the Appendix.

In Eq. (73), the intensities are given for transitions between the true molecular eigenstates, represented by the symmetrized rotational wavefunctions in Eqs. (3) and (10), rather than between the states represented by the functions in Eqs. (2) and (15). Consequently, the Boltzmann averaging necessitated by a given experimental arrangement does not involve any additional complications associated with using the signed angular momentum projections [38]. Instead, each intensity calculated from Eq. (73) needs only to be multiplied by $g\exp(-E/kT)$ where $g$ is the nuclear spin statistical weight.

The singlet-triplet spectrum of a polyatomic molecule is a very complicated matter, even for a symmetric top without the multiplet splitting. Therefore, our focus in this paper was to develop a general approach accompanied by a detailed derivation for a specific molecule, which is easily extendable to any other one. A more general formula is given in Appendix.

## 3. RESULTS AND DISCUSSION

### 3.1. The Correlation Diagram

A correlation diagram for the spin-rotational levels of the Hamiltonian (33) is shown in Fig. 2. For $\varepsilon = 0$ (no fine structure (FS) splitting) the levels of an asymmetric top are shown

as horizontal bars on the left-hand side of the diagram. The level labelling is $N_{K_{-1}K_{+1}}$, where the asymmetric top quantum number $K_{+1}$ reduces to the projection of the angular momentum N on the top axis $c$, $K_c$, in the limit of the oblate symmetric top ($A = B$). The asymmetry splitting for a nearly oblate symmetric top is first order in the small asymmetry parameter $A - B$ for $K_{+1} = 1$ and second order for $K_{+1} > 1$. Therefore, the splitting of the $2_{12}$ and $2_{02}$ levels is not seen at the energy scale of the figure. The symmetry species of the levels are shown in brackets.

Turning on the FS interaction ($\varepsilon > 0$) produces a splitting of all levels other than $N_{K_{-1}K_{+1}} = 0_{00}$, as shown in Fig. 2. Typically, three components are observed, corresponding to three possible values of $\mathbf{J} = \mathbf{N} + \mathbf{S}$. In general, the separation of the three components decreases with increasing $N$ (and $J$). The $J = 3$ components of the $2_{12}$ and $2_{02}$ levels remain nearly degenerate since their coupling is to the $3_{12}$ and $3_{22}$ levels, which lie at significantly higher energy. Each set of FS components belongs to the same symmetry species as the levels from which they are derived at $\varepsilon = 0$.

The spin levels of the nonrotating molecule and their correlation with the spin-rotational levels are shown in the right-hand side of the figure. The energy separations of the $T_{x,y,z}$ are arbitrary. A full correlation diagram would be two-dimensional, depending upon two parameters of the FS interaction Hamiltonian, $D$ and $E$ (see Eq. (16)). Instead, we show a one-dimensional section of the diagram, in which $D$ and $E$ are both proportional to $\varepsilon$ while their ratio, $E/D$, remains constant (see Eq. (33)). In this case the correspondence between the symmetry species of the spin-rotational levels and the pure spin levels is not defined uniquely, being dependent upon the value of $E/D$. Indeed, each spin-rotational wavefunction involves contributions from all three spin levels $T_{x,y,z}$ as is seen from the expansion (15) in the limit of $\varepsilon = 0$. When $\varepsilon > 0$, the same is true for the wavefunctions (34), where the relative contributions of $T_{x,y,z}$ depend on $\varepsilon$. In the limit of large $\varepsilon$, one of them dominates, but which one cannot be predicted without calculations since this depends on the $E/D$ ratio.

As an example, let us consider the $J = 1$ components of $2_{20}$, $2_{02}$, and $0_{00}$, which correlate with $T_z$, $T_y$, and $T_x$, respectively. If we change the sign of the FS constant $E$, the ordering of the levels $T_z$ and $T_y$ is reversed (see Eq. (18)). However, because of the non-crossing rule for terms of the same symmetry ($A$ in the present case), the previous correlation is not preserved. Instead, the $J = 1$ components of $2_{20}$, $2_{02}$, and $0_{00}$ now correlate with $T_y$, $T_z$, and $T_x$, respectively.

The number of levels with a given $J$ in Fig. 2 is equal to $6J + 3$, being defined by the usual momentum addition rule.

### 3.2. The Singlet-Triplet Spectrum of Pyrazine-$h_4$

We next used Eq. (73) to calculate the singlet-triplet absorption spectrum of the $0_0^0$ band of pyrazine-$h_4$. The spectrum was calculated by Boltzmann averaging the intensities of the individual transitions using a rotational temperature of 7 $cm^{-1}$ (10 K). The summation over the transitions was truncated at a maximum value of the total angular momentum $J_{max} = 12$, at which point the level populations were less than one percent of the total population. Nuclear spin statistical weights, $g(B_1) = g(B_3) = 9$, $g(B_2) = 13$, and $g(A) = 17$, were also taken into account. Each line was dressed with a Lorentzian whose full width at half maximum represents the resolution of the calculated spectra.

The spectra calculated with the parameters of Table 2 (and $\varepsilon = 1$ in Eq. (33)) are shown in Fig. 3. The top spectrum has the same resolution ($\sim 2$ GHz) as the published experimental spectra [25, 26]. The spectrum consists of a central intense $Q$ branch due to the $\Delta N = 0$ ($\Delta N \equiv N' - N''$) transitions, an $R$-form branch involving $R$ ($\Delta N = 1$) and $S$ ($\Delta N = 2$) transitions on

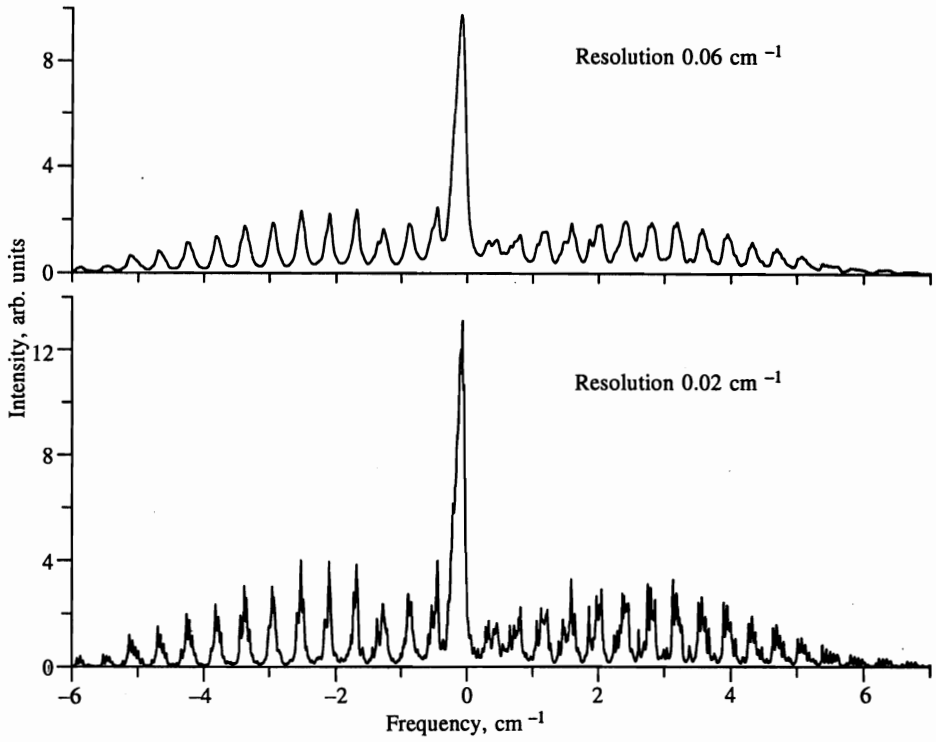


**Fig. 3.** The calculated singlet-triplet spectrum of pyrazine-$h_4$ at two different resolutions. The rotational temperature is $T_{rot}$ = 10 K, $J_{max}$ = 12

the high-frequency side of the $Q$ branch, and a $P$-form branch due to $O$ ($\Delta N = -2$) and $P$ ($\Delta N = -1$) transitions [25, 26] on the low-frequency side. At this level of resolution most of the individual bands in the $R$- and $P$-form branches of the calculated spectrum are structureless. Yet some splittings are seen, similar to those observed in the experimental spectra [25, 26]. For example, the $P(1)$ member has a shoulder on its red side, whereas $P(2)$ is structureless. $R(0)$ and $R(2)$ are weaker than $P(1)$ and exhibit more evident splittings.

The FS splitting becomes more pronounced in the spectrum calculated with a higher resolution of about 600 MHz (bottom panel in Fig. 3). The line splittings are more extensive in the $R$-form branch than in the $P$-form branch because transitions in the $R$-form branch access higher $J$ values in the triplet state.

The effect of the FS interaction on the spectrum is made more clear in Fig. 4 by the comparison of two spectra, one with $\varepsilon = 0$ and another with $\varepsilon = 1$. With $\varepsilon = 0$, the $R$-form branch is more intense than the $P$-form branch. Introducing the FS splitting decreases the overall intensity of each branch, but the effect on the $R$-form branch is larger since the degeneracy of the triplet levels for $R$ and $S$ transitions is higher than that for $P$ and $O$ transitions. Hence, the $R$- and $S$-type transitions are split into a larger number of components sharing the total intensity of a given transition. As a result, the intensities of the $P$- and $R$-form branches become more similar, and the spectrum acquires a sort of mirror image symmetry with respect to the $Q$ branch. Such a uniformity of high $J$ and low $J$ parts of the spectrum is expected from the fact that the rotational intervals are proportional to $2J$ and the rotational level degeneracy

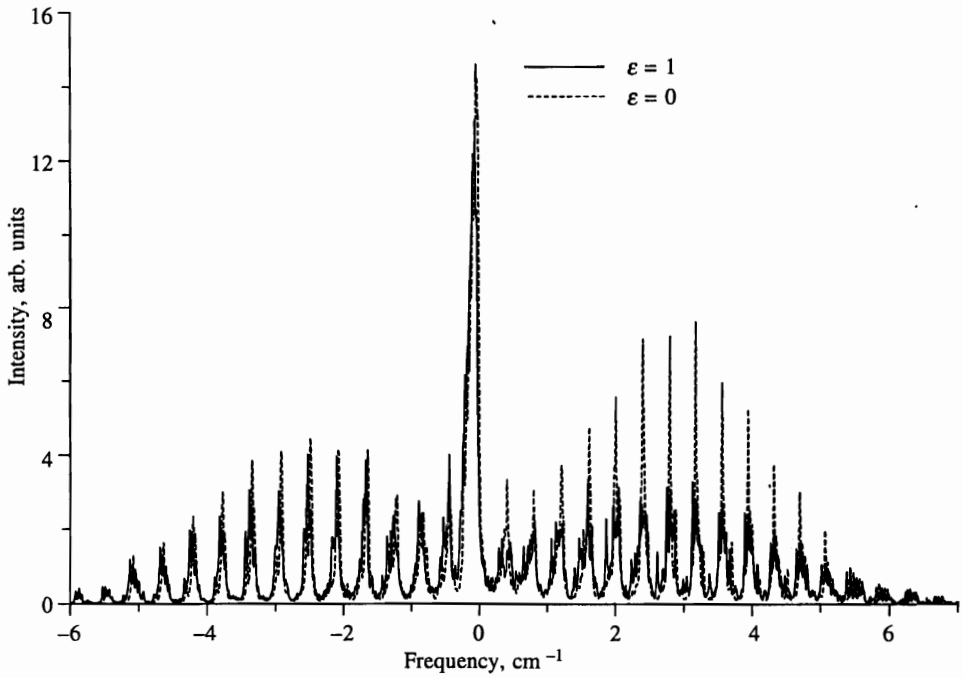


**Fig. 4.** Effect of fine structure splitting on the singlet-triplet spectrum of pyrazine. Resolution 0.02 $cm^{-1}$

to $2J + 1$, hence the density of states is essentially independent of $J$.

Figure 4 also clearly demonstrates the transition from Case ($a$) to Case ($b$) behavior. In both $P$-form and $R$-form branches, the low $J$ bands are split significantly, the splittings being on the order of the rotational band separations. This corresponds to Hunds's Case ($a$) coupling (or, more precisely, Case ($ab$), as noted earlier). With $J$ increasing, the splittings decrease and ultimately disappear in the high $J$ bands, characteristic of Case ($b$). Thus, we predict that Hund's Case ($a$) — Case ($b$) transition can be observed in as large a polyatomic molecule as pyrazine under quite moderate resolution conditions. The effect will also be observable in larger molecules, at higher resolution. Apart from the diatomic molecules mentioned in the Introduction, there have been no previous observations of this phenomenon in a polyatomic molecule. Recently, a pure Case ($ab$) spectrum has been reported in $H_2CSe$ [49].

Figure 5 shows the $R$-form branch on an expanded scale at higher resolution (150 MHz), to illustrate the relative importance of the asymmetry and FS splittings in pyrazine. The asymmetry splitting is more important for transitions terminating in $J \leq 4$, whereas the FS splitting is more important at higher $J$. Note, in Fig. 5$b$, that the asymmetry split bands still preserve their identity as rotational bands since the splittings are smaller than the band separations. In contrast, the FS splitting in Panel $c$ is large enough to fill the gaps between the low $J$ bands. Thus, these bands are actually spin-rotational rather than rotational in nature. Clearly, a high resolution of about 100 MHz will be required to observe this behavior. Even higher resolution ($\sim$ 10 MHz) will be required to observe the true molecular eigenstates.

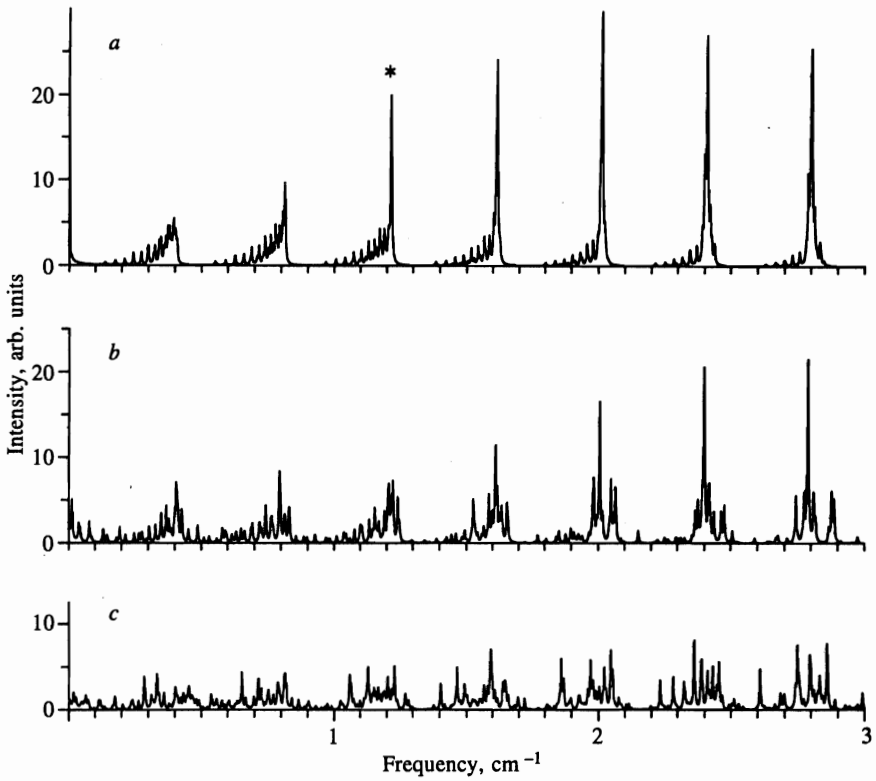


**Fig. 5.** Evolution of the $R$-form branch from a symmetric top with no fine structure splitting ($a$, $\varepsilon = 0$) to an asymmetric top with no fine structure splitting ($b$, $\varepsilon = 0$) to an asymmetric top with fine structure splitting ($c$, $\varepsilon = 1$). The starred band in panel $a$ involves degenerate $R(2)$ and $S(1)$ lines; these are split in panel $b$ due to asymmetry and further split in panel $c$ due to the spin-spin interaction. Resolution 0.005 cm$^{-1}$

### 3.3. The Singlet-Triplet Spectra of Pyrazine-$d_4$ and the Pyrazine-Ar van der Waals Complex

We also used Eq. (73) to calculate the singlet-triplet spectra of pyrazine-$d_4$ and the pyrazine-Ar van der Waals complex. Our objective was to compare these spectra with those of pyrazine-$h_4$, thereby exploring the effects of varying the magnitudes of the rotational constants on the Case ($a$) — Case ($b$) transition. In the calculation on pyrazine-$d_4$, we used the known rotational constants of the $S_0$ state (see Table 2) and assumed, for the $T_1$ state, that the rotational constants are reduced upon deuteration in the same proportion as in the $S_0$ state. The smallest moment of inertia in both states is now the moment about the $x$ axis [44]. Thus, the rotational constants $A$ and $B$ are exchanged in the Hamiltonian (1). The nuclear spin statistical weights are $g(B_1) = g(B_3) = 6$, $g(B_2) = 7$, and $g(A) = 8$ in this case. Taking these changes into account, we obtain the spectra shown in Fig. 6, with and without the FS splitting. Comparing the two spectra, we again see that turning on the FS splitting decreases the intensiy of the $R$-form branch relative to the $P$-form branch. We also note that numerous lines appear in the gaps between the rotational bands at low $J$, and that these lines disappear at high $J$. This behavior is again a manifestation of the Case ($a$) — Case ($b$) transition; turning on the rotation decouples the spin from the molecular frame and distributes the oscillator strength more uniformly, as

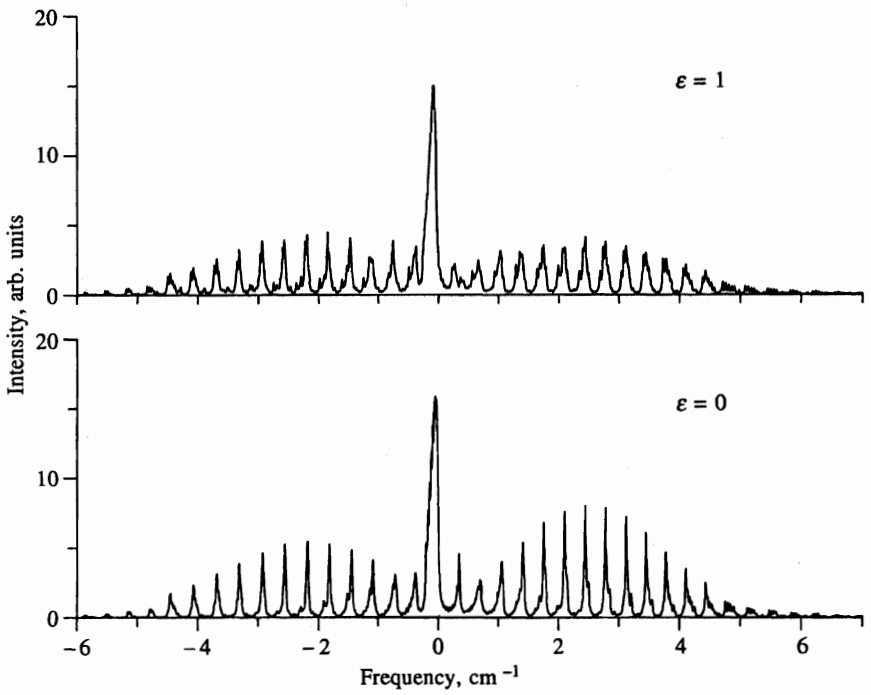


**Fig. 6.** The calculated singlet-triplet spectrum of pyrazine-$d_4$. Top panel, with fine structure splitting; bottom panel, without fine structure splitting. Resolution 0.01 $cm^{-1}$, $T_{rot}$ = 10 K

noted in Sect. 3.2.

The singlet-triplet spectrum of the pyrazine-Ar van der Waals complex has been observed in a supersonic jet using the MPI technique [19], at low resolution. No rotationally resolved spectra have been reported to date. To model such a spectrum, we assumed that the Ar atom lies on the $z$ axis perpendicular to the ring plane, at a distance of 3.5 Å, as it is in benzene-Ar [50] and $s$-tetrazine-Ar [51]. With this model, the $C$ rotational constant remains unchanged whereas the $A$ and $B$ constants are reduced by a factor of 4.8, in both states. The nuclear spin statistical weights are $g(A) = g(B_1) = 13$ and $g(B_2) = g(B_3) = 11$. The spectra calculated using these modified parameters are shown in Fig. 7.

Comparing the spectra for these species (Figs. 3, 6, and 7), we see first that the singlet-triplet spectrum of pyrazine-Ar is considerably more congested than those of the bare molecule, owing to the significant decrease in the values of $A$ and $B$. Still, the complex exhibits well-defined branches in its spectrum, in the absence of the FS interaction. However, turning on this interaction has a dramatic effect on the spectrum. The low $J$ rotational transitions, within $\pm 1$ $cm^{-1}$ of the $Q$ branch, are extensively mixed by the spin-spin coupling. Still, a defined level structure exists, although extremely high resolution ($\sim$ 1 MHz) will be required to expose the individual eigenstates. The long lifetime of the triplet state should permit such experiments in the near future, raising the intriguing probability of seeing still more underlying structure, including that due to hyperfine interaction and/or couplings to nearly isoenergetic ground state levels. The possibility of observing such effects is enhanced at high $J$ (cf. Fig. 7), where the structure with $\varepsilon \neq 0$ is even simpler than that with $\varepsilon = 0$, the transition to pure Case ($b$) being «complete».

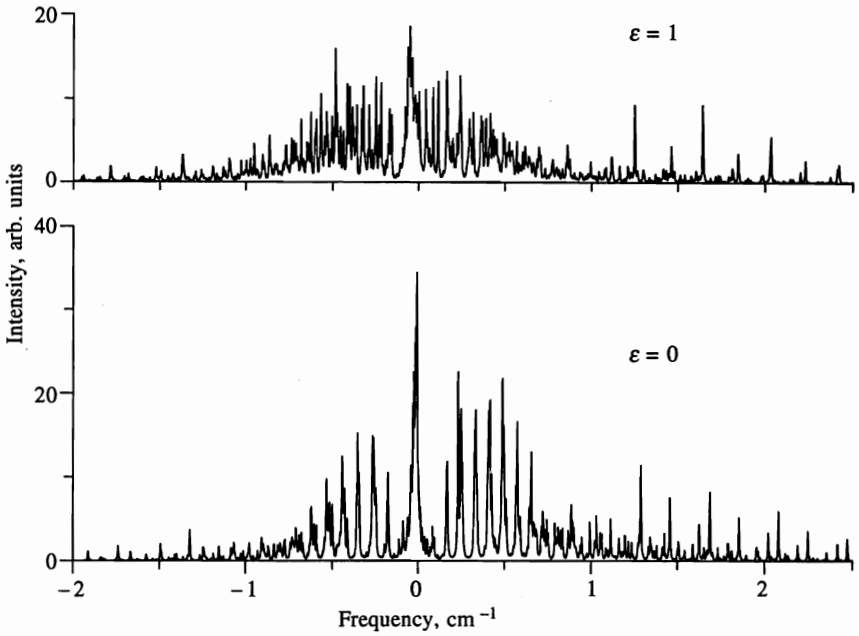


**Fig. 7.** The calculated singlet-triplet spectrum of the pyrazine-Ar van der Waals complex. Top panel, with fine structure splitting; bottom panel, without fine structure splitting. Resolution 0.005 $cm^{-1}$, $T_{rot}$ = 1.5 K

## 4. CONCLUSIONS

A closed-form analytical expression has been derived for calculating the intensities of individual spin-rovibronic lines in the singlet-triplet absorption spectrum of a polyatomic molecule. This expression takes into account both the intramanifold spin-spin coupling within the triplet state and the intermanifold spin-orbit coupling of the triplet to an excited singlet state. It also includes asymmetry splittings, and therefore can be applied to asymmetric tops as well as symmetric tops. With this expression, we have calculated the spectra of three species: pyrazine-$h_4$, pyrazine-$d_4$, and the pyrazine-Ar van der Waals complex, using the available experimental values of the gas-phase rotational and solid-state fine structure parameters of pyrazine-$h_4$ and model parameters for the remaining molecules. Comparison of the predictions of the theory with the available data for pyrazine-$h_4$ shows good agreement with experiment. The remaining molecules have not yet been examined at high resolution.

The computed spectra exhibit a number of interesting properties, the most notable being the transition from Case ($a$) to Case ($b$) with increasing $J$ and/or increasing molecular size. Inclusion of the fine structure interaction in the zero-order triplet state results in a decrease in the intensity of the $R$- and $S$-transitions, compared to $P$- and $O$-transitions branches, and a more symmetric spectrum. This effect has been observed in moderate resolution experiments [25, 26]. Additionally, spin-rotational transitions appear in the gaps between «pure» rotational transitions at low $J$, fragmenting the spectrum, but disappear at high $J$. This effect is more pronounced in pyrazine-$d_4$ and the pyrazine-Ar van der Waals complex, owing to their smaller rotational constants. All of the predicted behavior should be observable in experiments

performed with a resolution of $\leq 100$ MHz.

The analytical expression derived here can be used for interpretation of the singlet-triplet spectrum of any polyatomic molecule with arbitrary large (or small) rotational and fine structure constants.

This work was made possible in part by the US NAS/NRC CAST program, by grants № SDQ000 and NJ6000 from the International Science Foundation, grant № NJ6300 from the International Science Foundation and the Government of the Russian Federation. It was also supported by the Russian Foundation for Basic Research (project № 95-03-08130a) and the U. S. National Science Foundation (CHE-9617208).

## *APPENDIX*

### The general formula for the intensities and its relation to the Hougen factors

A general formula for the intensities can be derived from Eq. (62) if we represent the triplet function in the most general form, Eqs. (10) and (15), not invoking Eq. (53). Introducing the notation

$$\Omega_{\sigma'\sigma} = \langle \Gamma_T; 1\sigma' | \mu_\sigma^{(1)} | \Gamma_S \rangle, \tag{A.1}$$

we obtain

$$I(\Gamma_T \Gamma'_\tau \lambda' S' J' i' \leftarrow \Gamma_S \Gamma''_\tau \lambda'' \tau'' S'' J'' N'' i'') = \frac{1}{4}(2J'+1)(2J''+1) \times$$

$$\times \left| \sum_{N'=|J'-1|}^{J'+1} \sqrt{2N'+1} \sum_{\substack{K'=0 \\ \text{(only even or odd)}}}^{N'} f_{K'} C_{N'K'}^{(i')} \sum_{\substack{K''=0 \\ \text{(only even or odd)}}}^{J''} f_{K''} C_{K''}^{(i'')} \times \right.$$

$$\left. \times \sum_{P'=-J'}^{J'} \sum_{\sigma'\sigma=0,\pm 1} \Omega_{\sigma'\sigma} F_{P'\sigma'\sigma} \right|^2, \tag{A.2}$$

where $F_{P'\sigma'\sigma}$ is given by Eq. (74). The selection rules are the same as in Eq. (75), plus $\Delta K = \pm 1$. The rule $\lambda' = -\lambda''$ does not apply anymore.

A general expression for $\Omega_{\sigma'\sigma}$ found from Eqs. (41), (43), and (56) is

$$\Omega_{\sigma'\sigma} = \sum \frac{i}{\Delta E} c_{\sigma'}^{(1)*} \mu_\sigma^{(1)}, \tag{A.3}$$

where the star denotes a complex conjugate, $\mu_\sigma^{(1)}$ now stands for $\langle \Gamma_{S_n} | \mu_\sigma^{(1)} | \Gamma_S \rangle$, and the summation is over all contributing singlet states $S_n$. The following identity is easily derived either by applying the time reversal operator (14) or from the definition of the spherical tensors in Eq. (42):

$$\Omega_{-\sigma',-\sigma} = (-1)^{\sigma'+\sigma+1} \Omega_{\sigma'\sigma}^*. \tag{A.4}$$

For pyrazine, retaining a single term of the sum (A.3) and inserting Eqs. (45), (61), and (70), we find

$$\Omega_{\sigma'\sigma} = -\frac{1}{2}\sigma'|\sigma|\mu(B_{3g}). \tag{A.5}$$

In this case Eq. (A.4) reduces to

$$\Omega_{-\sigma',-\sigma} = -\Omega_{\sigma'\sigma}. \tag{A.6}$$

Designating the last sum in Eq. (A.2) by $A(P')$ and using Eq. (A.6) and the properties of 3-$J$ symbols in Eq. (74), we derive

$$A(-P') = -\lambda'\lambda'' A(P'). \tag{A.7}$$

Inserting this into the identity

$$\sum_P A(P) \equiv \sum_{P\geq 0} f_P^2 \left[A(P) + A(-P)\right] \tag{A.8}$$

folowing from Eq. (4), we immediately obtain the selection rule $\lambda' = -\lambda''$. Now, it is easy to verify that Eq. (A2) reduces to Eq. (73) in the particular case of pyrazine.

The intensities of individual rotational lines in the singlet-triplet spectrum of a symmetric top molecule without fine structure splitting were given by Hougen [38] in a tabular form for the $D_{2h}$ point symmetry group, together with directions for the use of these tables for other groups. Our general formula (A.2) enables us to derive a single unified expression embracing all cases considered by Hougen. In Eq. (A.2), one has to put

$$C^{i'}_{N'K'} = \delta_{i',N'K'} \quad \text{and} \quad C^{i''}_{K''} = \delta_{i'',K''},$$

and then to convert it to give the intensities for transitions between nonsymmetrized states (with $K'$ and $K''$ taking both positive and negative values). This is performed by a simple transformation of the transition amplitude from basis (3) to basis (2). The result reads

$$I(\Gamma_T J'N'K' \leftarrow \Gamma_S J''K'') = (2N'+1)(2J'+1)(2J''+1) \times$$
$$\times \left| \sum_{P'\sigma'\sigma} \Omega_{\sigma'\sigma} \begin{pmatrix} J' & 1 & N' \\ -P' & \sigma & K' \end{pmatrix} \begin{pmatrix} J' & 1 & J'' \\ -P' & \sigma' & K'' \end{pmatrix} \right|^2, \tag{A.9}$$

where the actual summation is performed only over $\sigma$ since $P' = \sigma + K'$ and $\sigma' = \sigma + \Delta K$; $\Delta K \equiv K' - K''$. The $3\times 3$ matrix (A.1) is expressed in terms of nine real intensity parameters, $\Omega_{ik}$, $i,k = x,y,z$, in the same manner as each member of the sum of Eq. (A.3) is expressed in terms of $c_i\mu_k/\Delta E$ using the definition (42). For instance,

$$\Omega_{00} = i\Omega_{zz}, \quad \Omega_{+1,-1} = \frac{1}{2}(-i\Omega_{xx} + i\Omega_{yy} - \Omega_{xy} - \Omega_{yx}), \tag{A.10}$$

etc. For the $D_{2h}$ group, our intensity parameters can be related to the Hougen parameters $\mu(B_{1g})$, $\mu(B_{2g})$, and $\mu(B_{3g})$ as shown in the following examples.

For $\Delta K = \Delta N = \Delta J = 0$, Eq. (A.9) gives

$$I = \frac{2J+1}{J^2(J+1)^2} \left| \frac{i}{2}(\Omega_{xx} + \Omega_{yy})\left[K^2 - J(J+1)\right] + i\Omega_{zz}K^2 - \frac{1}{2}(\Omega_{xy} - \Omega_{yx})K \right|^2, \tag{A.11}$$

where $K = K''$ and $J = J''$. Thus, in general, five intensity parameters govern this particular transition. In case of the ${}^3A_u \leftarrow {}^1A_{1g}$ transition in the $D_{2h}$ group, the possible contaminating singlets having nonzero transition moments $\mu_{x,y,z}$ from the ground state are ${}^1B_{3u}$, ${}^1B_{2u}$, and ${}^1B_{1u}$, respectively. The corresponding triplet sublevels acquiring the oscillator strength *via* the spin-orbit coupling parameters $c_{x,y,z}$ are $T_{x,y,z}$. Since the transformation rules for $\Omega_{ik}$ are the same as for $c_i\mu_k$, we obtain the following three nonvanishing parameters, assigning them Hougen's notations:

$$\mu(B_{1g}) = \Omega_{zz}, \quad \mu(B_{2g}) = -\Omega_{yy}, \quad \mu(B_{3g}) = \Omega_{xx}. \tag{A.12}$$

These definitions apply to all transitions with $\Gamma_S \times \Gamma_T = A_u$. Equations (A.9) and (A.12) entirely reproduce Hougen's Table 1, apart from an insignificant phase factor of the transition amplitude. Similarly, for $\Gamma_S \times \Gamma_T = B_{1u}$, two nonvanishing parameters are

$$\mu(B_{2g}) = -\Omega_{yx}, \quad \mu(B_{3g}) = \Omega_{xy}. \tag{A.13}$$

Equations (A.9) and (A.13) reproduce Hougen's Table 2. Pyrazine belongs here, with $\mu(B_{2g}) = 0$ (cf. Eqs. (A.5), (A.10), and (A.13)). For $\Gamma_S \times \Gamma_T = B_{2u}$ or $B_{3u}$, all five parameters vanish.

For $\Delta K = \Delta N = \Delta J = 1$ Eq. (A.9) gives

$$I = \frac{(J+K+1)(J+K+2)}{4(J+1)^2(J+2)} \left|(i\Omega_{xz} - \Omega_{yz})(J-K+1) + (i\Omega_{zx} - \Omega_{zy})(K+1)\right|^2. \tag{A.14}$$

For $\Gamma_S \times \Gamma_T = B_{2u}$ in the $D_{2h}$ group, the nonvanishing parameters are

$$\mu(B_{1g}) = \Omega_{zx}, \quad \mu(B_{3g}) = \Omega_{xz}. \tag{A.15}$$

Equations (A.9) and (A.15) reproduce Hougen's Table 3. Application of Eq. (A.9) to any other point group is straightforward; one has to calculate the intensity of a particular $\Delta K$, $\Delta N$, $\Delta J$ transition and then to define, by the usual rules, which of the intensity parameters vanish. For a molecule with no symmetry, all nine intensity parameters $\Omega_{ik}$ are present, but not all of them are relevant to a given transition. Thus, five parameters govern the intensity of the $\Delta K = \Delta N = \Delta J = 0$ branch, Eq. (A.11), and the other four govern the intensity of the $\Delta K = \Delta N = \Delta J = 1$ branch, Eq. (A.14).

## References


1. E. S. Medvedev and V. I. Osherov, *Radiationless Transitions in Polyatomic Molecules*, Springer, Berlin (1995).
2. O. Sekiguchi, N. Ohta, and H. Baba, Laser Chem. **7**, 213 (1987).
3. J. Kommandeur, W. A. Majewski, W. L. Meerts, and D. W. Pratt, Ann. Rev. Phys. Chem. **38**, 433 (1987).
4. J. Kommandeur, Adv. Chem. Phys. **70**(1), 133 (1988).
5. A. Amirav, J. Phys. Chem. **92**, 3725 (1988).
6. E. S. Medvedev, Uspekhi Fiz. Nauk **161**, 31 (1991).
7. E. S. Medvedev and D. W. Pratt, J. Chem. Phys. **105**, 3366 (1996).
8. *The Triplet State*, ed. by A. B. Zahlan, Cambridge University Press, Cambridge (1963).

9. D. M. Burland and J. Schmidt, Mol. Phys. **22**, 19 (1971).
10. M. A. El-Sayed, in *MTP International Review of Science*, Physical Chemistry Series 1, ed. by D. A. Ramsay, Butterworths, London (1972), Vol. 3, p. 119.
11. A. A. Gwaiz and M. A. El-Sayed, Chem. Phys. Lett. **19**, 11 (1973).
12. U. P. Wild, in *Triplet States*, Springer, Berlin (1975), Vol. 2.
13. H. Hirt, Spectrochim. Acta **12**, 114 (1958).
14. L. Goodman and M. Kasha, J. Mol. Spectrosc. **2**, 58 (1958).
15. R. M. Hochstrasser and C. Marzzacco, J. Chem. Phys. **49**, 971 (1968).
16. K. K. Innes and L. E. Giddings, Jr., Disc. Far. Soc. **35**, 192, 237 (1963).
17. A. E. Douglas and M. Milton, Disc. Far. Soc. **35**, 235 (1963).
18. G. Fisher, Chem. Phys. Lett. **79**, 573 (1981).
19. E. Villa, M. Terazima, and E. C. Lim, Chem. Phys. Lett. **129**, 336 (1986).
20. L. H. Spangler, Y. Matsumoto, and D. W. Pratt, J. Phys. Chem. **87**, 4781 (1983).
21. L. H. Spangler and D. W. Pratt, J. Chem. Phys. **84**, 4789 (1986).
22. L. H. Spangler, D. W. Pratt, and F. W. Birss, J. Chem. Phys. **85**, 3229 (1986).
23. J. L. Tomer, K. W. Holtzclaw, D. W. Pratt, and L. H. Spangler, J. Chem. Phys. **88**, 1528 (1988).
24. A. Penner and A. Amirav, J. Phys. Chem. **92**, 5079 (1988).
25. A. Penner, Y. Oreg, E. Villa, E. C. Lim, and A. Amirav, Chem. Phys. Lett. **150**, 243 (1988).
26. K. W. Holtzclaw, L. H. Spangler, and D. W. Pratt, Chem. Phys. Lett. **161**, 347 (1989).
27. O. Sneh, D. Dünn-Kittelplon, and O. Cheshnovsky, J. Chem. Phys. **91**, 7331 (1989); I. Becker and O. Cheshnovsky, J. Chem. Phys. **101**, 3649 (1994).
28. S. Hillenbrand, L. Zhu, and P. M. Johnson, J. Chem. Phys. **95**, 2237 (1991).
29. J. W. Sidman, J. Mol. Spectrosc. **2**, 33 (1958).
30. E. Clementi and M. Kasha, J. Mol. Spectrosc. **2**, 297 (1958).
31. L. Goodman and V. G. Krishna, Rev. Mod. Phys. **35**, 541, 735 (1963).
32. M. A. El-Sayed, in *Molecular Luminescence*, ed. by E. C. Lim, Benjamin, New York (1969), p. 715.
33. M. A. El-Sayed, J. Chem. Phys. **38**, 2834 (1963).
34. D. S. McClure, J. Chem. Phys. **20**, 682 (1952).
35. B. J. Cohen and L. Goodman, J. Chem. Phys. **46**, 713 (1967).
36. G. Herzberg, *Molecular Spectra and Molecular Structure. I. Spectra of Diatomic Molecules*, Van Nostrand, Princeton (1964), p. 231.
37. L. D. Landau and E. M. Lifshitz, *Quantum Mechanics*, 3rd ed., Pergamon, Oxford (1981), p. 319.
38. J. T. Hougen, Can. J. Phys. **42**, 433 (1964).
39. F. Creutzberg and J. T. Hougen, Can. J. Phys. **45**, 1363 (1967).
40. C. di Lauro, J. Mol. Spectrosc. **35**, 461 (1970).
41. J. H. Van Vleck, Rev. Mod. Phys. **23**, 213 (1951).
42. W. T. Raynes, J. Chem. Phys. **41**, 3020 (1964).
43. H. Sternlicht, J. Chem. Phys. **38**, 2316 (1963).
44. K. K. Innes, I. G. Ross, and W. R. Moomaw, J. Mol. Spectrosc. **132**, 492 (1988).
45. W. E. Howard and E. W. Schlag, in *Radiationless Transitions*, ed. by S. H. Lin, Academic, New York (1980), p. 81.
46. L. Goodman and V. G. Krishna, J. Chem. Phys. **37**, 2721 (1962).
47. P. R. Bunker, *Molecular Symmetry and Spectroscopy*, Academic, New York (1979).
48. D. A. Kleier, R. L. Martin, W. R. Wadt, and W. R. Moomaw, J. Am. Chem. Soc. **104**, 60 (1982).
49. D.-L. Joo, D. J. Clouthier, R. H. Judge, and D. C. Moule, J. Chem. Phys. **102**, 7351 (1995).
50. Th. Weber, A. von Bargen, E. Riedle, and H. J. Neusser, J. Chem. Phys. **92**, 90 (1990); Th. Weber and H. J. Neusser, J. Chem. Phys. **94**, 7689 (1991).
51. P. M. Weber and S. A. Rice, J. Chem. Phys. **88**, 6120 (1988).